Couette-Poiseuille flow of kerosene based ferrofluid in a rotating channel with mass transfer and slip effect

By

Seema Ahsan

MS THESIS
SESSION 2017-2019

Department of Computer Sciences
Bahria University, Islamabad Campus
2017-2019

hria University
overing Knowledge

MS-14A

Author's Declaration

I, **Seema Ahsan** hereby state that my MS thesis titled **"Couette-Poiseuille flow of kerosene based ferrofluid in a rotating channel with mass transfer and slip effect"** is my own work and has not been submitted previously by me for taking any degree from this university **Bahria University Islamabad** or anywhere else in the country/world. At any time if my statement is found to be incorrect even after my Graduate the university has the right to withdraw/cancel my PhD degree.

Name of scholar: **Seema Ahsan**

Date: **30-09-2019**

Bahria University
Discovering Knowledge

MS-14B

Plagiarism Undertaking

I, solemnly declare that research work presented in the thesis titled **"Couette-Poiseuille flow of kerosene based ferrofluid in a rotating channel with mass transfer and slip effect"** is solely my research work with no significant contribution from any other person. Small contribution / help wherever taken has been duly acknowledged and that complete thesis has been written by me.

I understand the zero tolerance policy of the HEC and Bahria University towards plagiarism. Therefore I as an Author of the above titled thesis declare that no portion of my thesis has been plagiarized and any material used as reference is properly referred / cited.

I undertake that if I am found guilty of any formal plagiarism in the above titled thesis even after award of PhD degree, the university reserves the right to withdraw / revoke my PhD degree and that HEC and the University has the right to publish my name on the HEC / University website on which names of students are placed who submitted plagiarized thesis.

Student / Author's Sign: 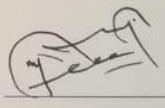

Name of the Student: **Seema Ahsan**

Bahria University
Discovering Knowledge

MS-13

Thesis Completion Certificate

Student's Name: **Seema Ahsan** Registration No. **34192**

Programme of Study: **MS(Mathematics)**

Thesis Title: **"Couette-Poiseuille flow of kerosene based ferrofluid in a rotating channel with mass transfer and slip effect"**

It is to certify that the above student's thesis has been completed to my satisfaction and, to my belief, its standard is appropriate for submission for Evaluation. I have also conducted plagiarism test of this thesis using HEC prescribed software and found similarity index at 18 % that is within the permissible limit set by the HEC for the MS/MPhil degree thesis. I have also found the thesis in a format recognized by the BU for the MS/MPhil thesis.

Principal Supervisor's Signature: _____

Date: 30-09-2019 **Name:** Dr. Jafar Hasnain

Dedicated to

*I am dedicating this thesis to my beloved sister **Neelam Aslam** who has meant a lot to me. Although she is no longer in this world. Her memories continue to regulate my life. Though your life was short, I will make sure your memory lives as long as my life shall live. May Almighty Allah grant you Jinnah Firdaws Ameen.*

Acknowledgment

In the name of Allah the most Merciful and Beneficent

First and foremost praise is to ALLAH, the Almighty, the greatest of all, on whom ultimately we depend for sustenance and guidance. Countless salutations be upon the Holy Prophet MUHAMMAD (PBUH) who ordained every Muslim to yearn for knowledge from cradle to grave. I would like to thank Almighty Allah for giving me opportunity, determination and strength to do my research. His continuous grace and mercy was with me throughout my life and ever more during the tenure of my research.

I'm deeply grateful to my supervisor **Dr. Jafar Hasnain**, who always providing his heartfelt support and guidance at all time and suggestion in my quest for knowledge and has given me invaluable guidance, inspiration throughout the session in Bahria University, Islamabad Campus. He has given me all the freedom to pursue my research, I consider myself very fortunate for being able to work under the supervision of such a kind person.

My acknowledgement would be incomplete without thanking the biggest source of my strength, my family and friends. The love and care of my Maa G **Gulshan Aslam**, the blessings of my parents **Mrs. Roquia Ahsan & Mr. Ahsan ul Haq**, the support of my brothers (**Inzamam-ul-Haq & Ejaz –ul-Haq**), sister (**Saima Bilal**), niece (**Ummaymah Bilal**), cousin (**Mehran Aslam**) and off course my prime source of courage my best friends **Asma Mubeen** & **Saiqa Gohar** who never let things get dull or boring, have made a tremendous contribution in helping me to reach this stage of my life. I thank all of them for putting up with me in difficult moments where I felt stumped and for goading me on to follow my dream. This would not have been possible without their unwavering and unselfish love and support given to me at all times.

SEEMA AHSAN
Bahria University
September 2019

Abstract

The aim of this thesis is to look into the problem of Couette-Poiseuille flow of kerosene based ferrofluid passing through rotating permeable channel. Heat and mass transfer analyses are carried out to see the behavior of ferrofluid in such situation. In this problem ferrofluid is subjected to the effects of magnetic field and velocity slip boundary condition. By means of transformations, the consequential governing equations are developed into coupled non-linear ordinary differential equations. By using shooting method, numerical results of these non-linear ordinary differential equations is attained. The physical impact of all fluid parameters on flow arenas are presented graphically and described in detail. The primary velocity of the fluid is discovered to increase by increasing the values of Reynolds numbers, magnetic parameters and slip parameters on the lower wall. However secondary velocity decreases with magnetic parameter. Also fluid temperature increases by rotation parameter, Eckert number and upper wall motion parameter. Mass transfer in the fluid increases by the greater value of Schmidt number along with chemical reaction parameter.

Contents

List of Tables

Nomenclature

V	suction/injection velocity
U	dimensionless velocity
U_0	upper wall velocity
u, w	velocity components
U, W	dimensionless velocity components
x, y, z	cartesian coordinate
L	channel length
T_1	upper wall temperature
T_f	hot fluid temperature
T	nanofluid temperature
Sh	Sherwood number
Re	suction/ injection Reynolds number
R_0	fluid rotation parameter
q_w	wall heat flux
q_m	wall mass flux
t	transpose of matrix
Pr	Prandtl number
J	electric current density
Nb	Brownian motion parameter
P	nanofluid pressure
Nt	thermophoresis parameter
Nu	Nusselt number
Le	Lewis number
k	thermal conductivity
h_f	heat transfer coefficient
Ec	Eckert number
D_T	thermophoresis diffusion coefficient

D_B	Brownian diffusion coefficient
C_{pf}	specific heat and constant temperature
C_f	skin friction
C	nanoparticles connection
C_1	upper wall concentration
C_0	lower wall concentration
Bi	Biot number
B_0	strength of applied magnetic field
L^*	velocity gradient
k_n	reaction rate of the nth-order homogeneous chemical reaction.
A_1^*	first Rivlin-Erickson tensor
m	hall current parameter
Sc	Schmidt number
n_p	shape factor

Greek letters

ω_e	cyclotron frequency
τ_e	electron collision time
τ	ratio between heat capacity of nanoparticles and fluid
Ω	angular velocity
α_f	thermal diffusivity coefficient
λ	upper wall motion
δ	variable viscosity coefficient
β	viscosity variation parameter
η	dimensionless variable
θ	dimensionless temperature

ϕ	dimensionless concentration
μ	dynamic viscosity
υ	kinematic viscosity coefficient
σ	electrical conductivity
α_{nf}	thermal diffusivity
ρ_{nf}	effective density
μ_{nf}	effective dynamic viscosity
$\left(\rho C_p\right)_{nf}$	heat capacitance
κ_{nf}	thermal conductivity
φ	volume fraction
μ_f	dynamic viscosity
ρ_f	density for ferrofluid
ρ_s	density for base fluid
$\left(C_p\right)_f$	specific heat parameter
κ_f	thermal conductivity
$\left(C_p\right)_s$	specific heat parameter
κ_s	thermal conductivity for base fluid
α	slip parameter
φ	nanoparticle volume fraction
γ	Chemical Reaction parameter

List of Figures

Chapter 1

Introduction

1.1 Overview

The foremost purpose of this chapter is to emphasize on associated fundamental definitions and laws that describe the flow phenomena in a channel made by two infinite parallel walls viz. continuity, heat, mass transfer and momentum. The fundamental concepts of techniques for solving the governing equations are also presented.

1.2 Fluid

Fluid is a matter that can flow and which cannot have any specific shape. Some aspects of fluid flow are fluid evenness, fluid squeezability and fluid spinning. Fluid flow rely on the viscosity of fluid. Amount of a fluid's confrontation to flow is called viscosity. There are two kinds of fluid i.e. Newtonian and non-Newtonian fluid. Newtonian fluids are described by relation in shear rate & shear stress with a simple linear relation. But when a fluid does not satisfy the viscosity's law then it is known as non-Newtonian. Viscosity of non-NF is dependent on shear rate. Because the earth is 75% water-covered and 100% air-covered, there is a huge range of fluid mechanics and almost every human effort touches. Meteorology, physical oceanography and hydrology sciences are connected with natural fluid flows. They are extensively employed in food & nutrients industry, petroleum industry, chemical engineering, biological interpretation as well as some other fields.

1.3 Nanofluid

Nanofluid (NF) is a liquid that contains particles of nanometer size called nanoparticles (NPs). These kinds of fluids are produced in a base fluid with colloidal

suspensions of NPs. The NPs utilized in nanofluids (NFs) are ordinarily made of oxides and metals. Normal base liquids are oil and water. NFs have different properties that are helpful in various solicitations in heat exchange, energy units, microelectronics, medical procedures, crossover fueled motors, local fridge, heat exchanger, chiller, atomic reactor coolant, in granulating, machining and in space innovation. There are different models that can best describe the characteristics of NFs. One of them is a Buongiorno fluid model. Buongiorno model examines the reaction of Brownian motion and thermophoresis on flow, mass and heat transfer.

1.4 Ferrofluid

Another type of NF is ferrofluid (FF) which turns out to be highly charged within the sight of a magnetic field. FFs contain nanoscale ferromagnetic or ferrimagnetic particles in a transporter liquid. These two liquids have altogether different applications subsequently. The characteristics of FF make it beneficial for various applications. In computer hard drives and other rotating shaft engines, FF is used in rotating seals. To dampen vibrations, laoudspeakers use FF. As a contrast agent for magnetic resonance imaging (MRI), FF is used in medicine.

1.5 Hall effect

The Hall effect (HE) is the creation of an electrical conductor voltage difference, transverse to an electrical current in the conductor and perpendicular to the current to an applied magnetic field. HE is also used in bicycle wheels and some electronic types of systems e.g. electronic campuses. Now a days mostly HE are used in smart phones, as well as in some guns and GPS systems. Moreover, HE analogue multiplication application is used in small computers.

1.6 Mass transfer

Mass transfer is an imperative procedure as a result of its appearance in a few logical controls that require convective exchange of molecules and atoms. Mass exchange has two fundamental types i.e. purely diffusive mass transfer and convective mass transfer. It is experienced in chemical procedure in both building and partition forms. Periodically, a chemical procedure might be utilized to quicken the mass transport rate. In this regard, Lorentz force is the very important part used to control the stream in such circumstances. On the other hand, in several chemical engineering procedures, mixed mass and heat transfer, chemical reaction problems are excellent significance, thus attracting significant attention in latest years.In addition, chemical reactions have usually been categorized as homogeneous and heterogeneous. The chemical engineering which is shown in the principle part of the fluid, it has various compound structure and present-day applications such as in the gathering of stoneware generation, polymer creation, sustenance getting ready, etc.

1.7 Magnetohydrodynamics

Magnetohydrodynamics (MHD) is the study of the magnetic characteristics and behavior of the liquids. Rotating flow of MHD viscous fluids has huge applications in astrophysics, industrial design and geophysics. MHD play a key role in evaluating the mass ejections, corona structure and triggering solar flares.

1.8 Slip flow

In the no slip flow regime, the relative speed of the liquid and the wall is zero. But the relative speed is non-zero at the surface in the case of slip flow. There are numerous conditions when the liquid is particulate like polymer solutions and emulsion suspension and at that point slip condition is more suitable.

1.9 Basic Laws

The basic equations with heat exchange explaining the fluid flow are as under:

1.1.1 Equation of continuity

The continuity equation for incompressible fluid is

$$\nabla.\boldsymbol{V} = 0. \tag{1.1}$$

1.1.2 Conservation of momentum equation

$$\rho\mathbf{b}.\left(\boldsymbol{V}\cdot\nabla\right)\boldsymbol{V} + \mathrm{div}\boldsymbol{\tau} + 2\boldsymbol{\Omega}\times\boldsymbol{V} = \nu\nabla^2\boldsymbol{V} + \frac{1}{\rho}\ \mathbf{J}\times\boldsymbol{B} - \frac{1}{\rho}\nabla p = \rho\frac{d\,\mathbf{V}}{dt}, \tag{1.2}$$

together with the generalized law of Ohm, which takes into consideration the present Hall

$$\boldsymbol{j} + \left(\mathbf{j}\times\boldsymbol{B}\right)\frac{\omega_e\tau_e}{\beta_o} = \sigma\left(\boldsymbol{q}\times\boldsymbol{B} + \boldsymbol{E}\right). \tag{1.3}$$

1.1.5 Conservation of energy equation

$$\rho\boldsymbol{c}_p\left(\frac{\mathrm{dT}}{\mathrm{dt}}\right) = -div\boldsymbol{q} + \tau^*\cdot\boldsymbol{L}^*, \tag{1.4}$$

Here

$$\boldsymbol{\tau}* = \mu\boldsymbol{A}_1^* - p\boldsymbol{I}^*, \tag{1.5}$$

$$\boldsymbol{A}_1^* = \nabla\boldsymbol{V} + \left(\nabla\boldsymbol{V}\right)^t. \tag{1.8}$$

1.1.6 Concentration equation

$$\frac{dC}{dt} = D\nabla^2C + k_nC^n. \tag{1.9}$$

1.10 Solution methods

Differential equations (ordinary and partial differential) are commonly used in architecture and technological innovative world problems. Because of long lasting nonlinearity, this is

simply not possible to solve these types of equations. By the use similarity transformations, ordinary differential equations (ODEs) are derived from partial differential equations (PDEs) that can be further solved numerically. The basic way of the method used to solve the present problem is appended below.

1.10.1 Runge-Kutta Method

Several numerical methods are available to solve the ODEs by the use IVP (initial value problems). C. Runge and W. Kutta (German Mathematicians) presented precise as well as successful computational techniques named as Runge-Kutta (R-K) techniques. Out of all, fourth order R-K technique is more productive. Mostly, IVP of second order is articulated as

$$y'' = h\left(x^*, y^*, (y^*)'\right), \tag{1.10}$$

with initial condition

$$y^*\left(x^*_a\right) = y^*_a, \quad \left((y^*)\right)'\left(x^*_a\right) = c \tag{1.11}$$

By defining equation (1.10) as

$$y' = z = l\left(x^*, y^*, z^*\right), \tag{1.12}$$

and

$$z' = h\left(x^*_o, y^*_o, z^*_o\right), \tag{1.13}$$

and the initial conditions (ICs) are

$$y^*\left(x^*_a\right) = y^*_a, \quad z^*\left(x^*_a\right) = c \tag{1.14}$$

For Eqs (1.3) and (1.4), the R-K method is defined as under:

$$y^*_{j+1} = y^*_j + \frac{1}{6}\left(t_1 + t_2 + t_3 + t_4\right), \tag{1.15}$$

and

$$z_{j+1} = z_j + \frac{1}{6}\left(s_1 + s_2 + s_3 + s_4\right), \tag{1.16}$$

where

$$t_1 = gl\left(x^*_j, y^*_j, z^*_j\right), \qquad s_1 = gh\left(x^*_j, y^*_j, z^*_j\right),$$

$$t_2 = gl\left(x^*_j + \frac{h}{2}, y^*_j + \frac{t_1}{2}, z^*_j + \frac{s_1}{2}\right),\ s_2 = gh\left(x^*_j + \frac{h}{2}, y^*_j + \frac{t_1}{2}, z^*_j + \frac{s_1}{2}\right),$$

$$t_3 = gl\left(x^*_j + \frac{h}{2}, y^*_j + \frac{t_2}{2}, z^*_j + \frac{s_2}{2}\right),\ s_3 = gh\left(x^*_j + \frac{h}{2}, y^*_j + \frac{t_2}{2}, z^*_j + \frac{s_2}{2}\right),$$

$$t_4 = gl\left(x^*_j + h, y^*_j + t_3, z^*_j + s_3\right), \qquad s_4 = gh\left(x^*_j + h, y^*_j + t_3, z^*_j + s_3\right),$$

where g is the step size identified as

$$g = \frac{x^*_{n_0} - x^*_{0}}{n_0}. \tag{1.17}$$

In Eq. (1.17), step size is n_0, x^*_n is the last value and x^*_0 is initial value.

1.10.2 Shooting method

One of the numerical techniques used to fix that problem of the two-point limit value is known as the method of shooting. In this technique, by assuming the unknown conditions, the boundary value problem (BVP) of greater order is first changed to an IVP. In fluid mechanics and mathematical physics, shooting technique practice as an important method. The subject of the third order boundary value is regarded:

$$u''' = \Phi\left(u', u'', y^*, u^*\right), \tag{1.18}$$

with BCs

$$u'(0)^* = 0,\ u'(g) = A,\ u(0)^* = \alpha^*. \tag{1.19}$$

Here $y = 0$ to $y = g,$ is solution domain for Φ and unknown IC is considered as

$$u''(0) = r_1. \tag{1.20}$$

Eq. (1.18) is reducing as

$$u' = v, \tag{1.21}$$

$$v' = w, \tag{1.22}$$

$$w' = f\left(y, u, v, w\right), \tag{1.23}$$

whereas the ICs for above equations are follows

$$v(0) = 0,\ u(0) = \alpha_1 \text{ and } w(0) = r_1. \tag{1.24}$$

By differentiating Eqs. (1.23) - (1.24) w.r.t. r_1 like

$$v' = f' \times W + f' \times V + f' \times U, \tag{1.25}$$

where

$$U = \frac{\partial}{\partial r_1}(u), \mathrm{W} = \frac{\partial}{\partial r_1}(w), \mathrm{V} = \frac{\partial}{\partial r_1}(v), \tag{1.26}$$

and

$$V(0) = 0, U(0) = 0, W(0) = 1. \tag{1.27}$$

As Eq. (1.23) and Eq. (1.25) represent the two systems of IVP with initial conditions (1.24) and (1.27). The assumed value of r_1 must meet the requirement $u'(h) = \beta$ or $u(y, \mathrm{r}_1)$, $v(y, \mathrm{r}_1)$ and $w(y, \mathrm{r}_1)$ may expressed the results of initial value problems (IVP), one looks for the value of r_1 such that

$$\theta_1(r_1) = -\beta + u(\mathrm{g}, \mathrm{r}_1) = 0, \quad \text{(say)} \tag{1.28}$$

With the help of Newton's method, r_1 can be upgraded as

$$r_1^{(j+1)} = r_1^{(j)} - \frac{\theta_1\left(r_1^{(j)}\right)}{\theta_1'\left(r_1^{(j)}\right)}. \tag{1.29}$$

Putting $u(h, \mathrm{r}_1) - \beta = 0 = \theta_1(r_1), \quad \text{(say)}$ in Eq. (1.19), we get

$$-\frac{\left(u\left(h, \mathrm{r}_1^{(j)}\right) - \beta\right)}{\frac{\partial u}{\partial r_1}\left(h, \mathrm{r}_1^{(j)}\right)} + r_1^{(j)} = r_1^{(j+1)}. \tag{1.30}$$

Eqs. (1.21) – (1.23) with Eq. (1.27) are explained as under:

(i) The r_1 is selected as missing IC in Eq. (1.21) and symbolizing it by $r_1^{(1)}$

(ii) Eqs. (1.21) – (1.23) by the ICs (1.27) is integrated 0 to g.

(iii) with ICs (1.25) the Eq. (1.23) is solved as an IVP from 0 to g.

(iv) Substituting $u\left(\mathrm{g}, \mathrm{r}_1^{(1)}\right)$ & $U\left(\mathrm{g}, \mathrm{r}_1^{(1)}\right)$ in Eq. (1.28) we get

$$r_1^{(2)} = r_1^{(1)} - \frac{\left[u\left(\mathrm{g}, \mathrm{r}_1^{(1)}\right) - \beta \right]}{U\left(\mathrm{g}, \mathrm{r}_1^{(1)}\right)}.$$

(v) All above options are recurrent while the solution meets the condition of the specified limit.

Chapter 2

Literature Review

2.1 Overview

In this chapter we represented the literature study related to nanofluid, Hall effect, mass transfer, MHD and slip flow.

2.2 Related work

The NPs utilized in nanofluids (NFs) are ordinarily made of oxides and metals. Choi [1] investigated NFs and also indicated that they have novel physical substantial attributes and the particles within it possess higher thermal conductivities. Seo et al. [2] studied that thermal flow qualities of a FF in the existence of magnetic field. Goharkan [3] explained the constrained convective heat exchange of water-based FF exposed to variable magnetic field. Impact of magnetic field on basic heat motion of FF flow bubbling in an upright annulus explored by Aminfar et al. [4]. Murshed and Estelle [5] presented an inclusive review on analysis and progression along with features of NFs for their innovative heat transport applications. Iftikhar et al. [6] firstly focused on measuring mass diversity in NFs though in the second phase they concentrated on convective mass exchange in NFs. Qiang and Xuan [7] investigated the flow possessions of Cu-water NF, friction factor of cu-water NF and convective 1heat transfer for turbulent & laminar flow under the single phase flow and discovered the new convective heat transfer association established in tubes for NF. Ganji and Sheikholeslami [8] investigated FF flow and thermal transfer phenomena through the semi-annulus magnetic field enclosure. Ganji and Sheikholeslami [9] again addressed the nature of NF flows through differential conversion methods between Brownian movement and heat transfer between parallel plates. Together with thermal

radiation in a channel, Kandelousi & Mahmoodi [10] explored the heat transfer and Kerosene−alumina nanofluid flow with the presence of magnetic field. Fakour et al. [11] examined both NF flow and heat exchange across a channel.

The Hall effect is the production of Hall voltage normal to both the magnetic field and current by means of a magnetic field carrier. With the presence of HE, Attia et al. [12] investigated the impact of uniform magnetic field for transient Couette flow of a non-Newtonian Bingham fluid. Priyadarsan et al. [13] researched that, owing to Hall parameters, the velocity reduces and the skin friction coefficient increases. When a magnetic field is applied, the induction of strong magnetic field results in complicated phenomena along with Hall currents (HC), Joule's heating etc, as Cramer and Pai [14] have stated in an electrical flow regime. The Hall effects on free and forced convective rotating flow was examined by Rao and Krishna [15]. Attia [16] studied the effect of HC on Couette–Poiseuille (CP) flow of viscoelastic fluid owing to heat transfer. Chauhan and Agrawal [17] researched that the Hall current effects on MHD flow in a partly filled rotating channel with a porous medium. The HC and rotation impacts reported by Sarkar et al. [18] on steady hydromagnetic CP flow. Jha and Apere [19] are explored combined effects of HC in a rotating channel with ion-slip present on MHD CP flow. Makinde et al. [20] investigated numerically the MHD CP flow of variable viscosity NF with mass and heat transfer through parallel walls.

Mass transfer is an imperative procedure as a result of its appearance in a few logical controls that require convective exchange of molecules and atoms. Fang et al. [21] presented the experimental study on mass transfer in NF. Seth and Nandkeolyar [22] claimed that angle of inclination accelerates primary and secondary flow at the same time magnetic field retards it. Serna [23] with the help of heat and mass transfer studied the heat properties in steady two-dimensional NFs boundary layer. Singh and Chamkha [24] studied for second order slip flow over a continually permeable shrinking wall. Ojjela and Kumar [25] investigated the mass and heat exchange of micropolar fluid flow across a channel in the presence of Ion slip and Hall current. Fakour et al. [26] presented the solution of chemical reaction for micropolar fluid flow through the channel analytically as well as numerically. Tetbirt et al. [27] studied the micropolar fluid flow with magnetic field and convective heat exchange of viscous flued in vertical channel by using numerical analysis.

Ali et al. [28] examined the problem of the presence of a magnetic field over a folding sheet for an incompressible viscous fluid of the continuous stagnation point MHD. Makinde and Onyejekwe [29] investigated MHD generalized Couette flow and heat transfer numerically. Several writers [30–34] described regular / NF thermal exchange hydromagnetic flow in different geometries. Fersadou et al. [35] claimed that the flow of NF flow with magnetic field in a vertical channel. Many researchers about MHD in near past has been presented in [36-38].

There's a lot of conditions when the liquid is particulate, such as suspension emulsion, polymer solutions and froth, at that point slip condition is more suitable. In this regard, various authors were presented their research work such as Wang [39] studied the slip effects over an extending sheet for the flow of viscus fluid. Aziz [40] studied the impact of slip over flat plate in the flow of the boundary layer. The variation of velocity and thermal slip condition on the flow of eclectically conducting fluid past a sheet investigated by Hayat et al. [41]. Abbas et al. [42] were presented the analytic study on two phase flow of FF and viscous fluid in an inclined channel with slip velocity. The variety of slip impacts on NF flow past a sheet was discussed by Nandy and Mahpatra [43]. For some relevant studies readers are referred to see [44-50].

Chapter 3

Hall effects on Couette-Poiseuille flow of MHD nanofluid in a rotating channel with variable viscosity

3.1 Introduction

This chapter describes the hydromagnetic CP flow of NF with mass transfer through parallel plates. Brownian motion, thermophoresis, Joule heating, Hall effects and viscous dissipation are included in the nonlinear model describing this problem. The acquired equations are solved numerically by the aid of fourth order R–K integration system. The consequences of numerous parameters are also examined via graphs. This chapter is a review of the paper by Makinde et al. [20].

3.2 Problem development

Assumed two parallel walls, through which we have an incompressible electrically and thermally conducting NF with magnetic field B_0 applied transversely to the flow. Both the NF and channel rotate about y -axis with Ω. In this channel, flow is generated due to the combined action of applied pressure gradient along x -axis, the uniform motion of the upper wall U_0. The upper wall temperature is T_1 and lower wall is T_f with heat coefficient h_f. In this chapter, heat transfer investigation is also utilized with the help of Brownian motion. Figure. 3.1 represent fluid flow model. Since channel walls are infinite in x and z -directions, all parameters depend on y except pressure.

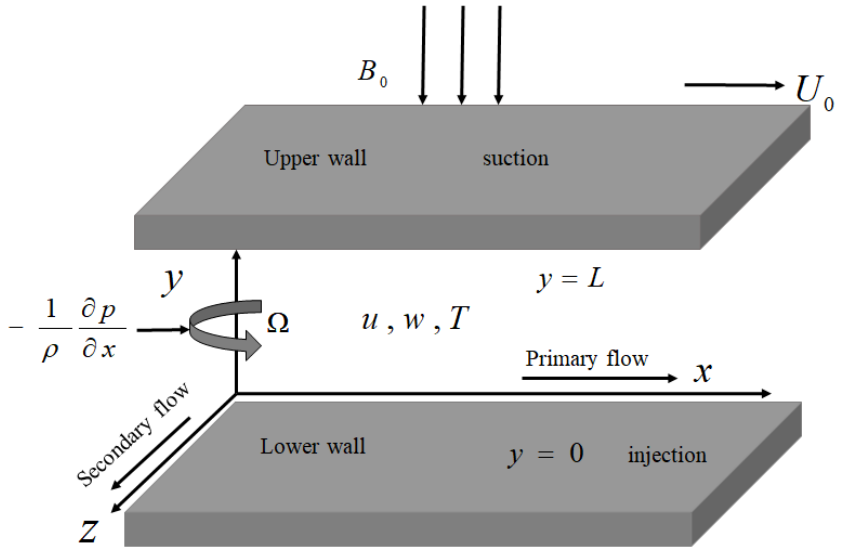

Figure.3.1: Fluid flow model

In view of above, following the Buongiorno [51] the main equations are given as

$$-V\frac{du}{dy}+2w\Omega=\frac{1}{\rho_f}\frac{d}{dy}\left(\mu_f\frac{du}{dy}\right)-\frac{\sigma B_0{}^2\left(u-U_0+mw\right)}{\rho_f\left(1+m^2\right)}, \tag{3.1}$$

$$-V\frac{dw}{dy}-2\Omega\left(u-U_0\right)=\frac{1}{\rho_f}\frac{d}{dy}\left(\mu_f\frac{dw}{dy}\right)-\frac{\sigma B_0{}^2\left(w-mu+mU_0\right)}{\rho_f\left(1+m^2\right)}, \tag{3.2}$$

$$-V\frac{dT}{dy}=\alpha_f\frac{d^2T}{dy^2}+\frac{\mu_f}{(\rho c_p)_f}\left(\left(\frac{du}{dy}\right)^2+\left(\frac{dw}{dy}\right)^2\right)+\frac{\sigma B_0{}^2}{\left(\rho c_p\right)_f}\left(\frac{(u-U_0+mu)^2+(w-mu+mU_0)^2}{\left(1+m^2\right)^2}\right)$$

$$-\tau\left(D_B\frac{dT}{dy}\frac{dC}{dy}+\frac{D_T}{T_f}\left(\frac{dT}{dy}\right)^2\right), \tag{3.3}$$

$$-V\frac{dC}{dy}=D_B\frac{d^2C}{dy^2}+\left(\frac{D_T}{T_f}\right)\left(\frac{d^2T}{dy^2}\right). \tag{3.4}$$

The dynamical viscosity is the function of temperature which is

$$\mu(T)=e^{-\beta(-T_f+T)}\mu_0. \tag{3.5}$$

The BCs are as under

$$u = w = 0, C = C_0, -k\frac{dT}{dy} = h_f(T_f - T),\ at\ \ y = 0,$$
$$u = U_0 T = T_1, C = C_1, w = 0, \text{at } y = L. \tag{3.6}$$

The dimensionless variables are used to make equation dimesionless

$$\eta = \frac{y}{L},\ X = \frac{x}{L},\ \theta = \frac{-T_f + T}{-T_f + T_1},\ \phi = \frac{-C_0 + C}{-C_0 + C_1},\ \delta = \beta(-T_f + T_1),\ \upsilon = \frac{\mu_0}{\rho_f},$$
$$U = \frac{uL}{\upsilon},\ W = \frac{wL}{\upsilon},\ Bi = \frac{Lh_f}{k},\ \text{Pr} = \frac{\upsilon}{\alpha_f},\ \alpha_f = \frac{k}{(\rho c_p)_f},$$
$$Ec = \frac{\upsilon}{C_{pf}(T_1 - T_f)L^2}, M = \frac{L^2 \sigma B_0^2}{\mu_0},\ R_0 = \frac{\Omega L^2}{\upsilon},\ Nb = \frac{\tau(C_1 - C_2)D_B}{\upsilon}, \tag{3.7}$$
$$\overline{P} = \frac{PL^2}{\rho_f \upsilon^2},\ Le = \frac{\alpha_f}{D_B},\ Nt = \frac{\tau D_T (T_1 - T_f)}{T_f \upsilon},\ \lambda = \frac{U_0 L}{\upsilon},\ \text{Re} = \frac{VL}{\upsilon}.$$

Now putting Eq. (3.7) into Eqs. (3.1) – (3.6), we get

$$-\text{Re}\frac{dU}{d\eta} + 2RoW = e^{-\delta\theta}\frac{d^2U}{d\eta^2} - \delta e^{-\delta\theta}\frac{d\theta}{d\eta}\frac{dU}{d\eta} - \frac{M\left(U - \lambda + mW\right)}{\left(1 + m^2\right)}, \tag{3.8}$$

$$-\text{Re}\frac{dU}{d\eta} - 2Ro\left(U - \lambda\right) = e^{-\delta\theta}\frac{d^2W}{d\eta^2} - \delta e^{-\delta\theta}\frac{d\theta}{d\eta}\frac{dU}{d\eta} - \frac{M\left(W - mU + m\lambda\right)}{\left(1 + m^2\right)}, \tag{3.9}$$

$$\frac{d^2\theta}{d\eta^2} + Re\,\text{Pr}\frac{d\theta}{d\eta} + Nb\frac{d\varphi}{d\eta}\frac{d\theta}{d\eta} - \left(\frac{d\theta}{d\eta}\right)^2 Nt + \text{Pr}\,Ec\left(\left(\frac{dW}{d\eta}\right)^2 + \left(\frac{dU}{d\eta}\right)^2\right)e^{-\delta\theta} +$$
$$\text{Pr}\,EcM\left(\frac{\left(U - mW + \lambda\right)^2 + \left(W - m\lambda + mU\right)^2}{\left(1 + m^2\right)^2}\right) = 0, \tag{3.10}$$

$$\frac{d^2}{d\eta^2}(\phi) + \text{Pr}\,Le\,\text{Re}\frac{d}{d\eta}(\phi) + \frac{Nb}{Nt}\frac{d^2}{d\eta^2}(\theta) = 0, \tag{3.11}$$

with BCs

$$W(0) = U(0) = 0,\ \frac{d\theta}{d\eta}(0) = \theta(0)Bi,\ \phi(0) = 0,$$
$$W(1) = 0,\ U(1) = \lambda,\ \theta(1) = \phi(1) = 1. \tag{3.12}$$

The special cases for Eq. (3.8) are also studied and solution of these cases are presented.

Case 1: Where $\delta = \text{Re} = M = Ro = 0,$ Eq. (3.8) becomes

$$U^{''}(\eta) = 0, \tag{3.13}$$

with BCs

$$U(1) = U(0) = \lambda. \tag{3.14}$$

The exact solution of Eq. (3.13) from 3.14

$$U = \eta\lambda\,. \tag{3.15}$$

Case 2: When $\delta = m = Ro = Re = 0,$ Eq. (3.8) becomes:

$$U^{"}(\eta) - M(U - \lambda) = 0\,, \tag{3.16}$$

with Eq. (3.14).

The solution of Eq. (3.16) is

$$U = \lambda\left(-\frac{e^{\sqrt{M}(1-\eta)}}{\left(-e^{-\sqrt{M}} + e^{\sqrt{M}}\right)} + \frac{e^{\sqrt{M}(\eta-1)}}{\left(-e^{-\sqrt{M}} + e^{\sqrt{M}}\right)} + 1\right). \tag{3.17}$$

Case 3. When $\delta = M = Ro = 0,$ Eq. (3.8) becomes:

$$U^{"}(\eta) + ReU^{'}(\eta) = 0, \tag{3.18}$$

with Eq. (3.14).

Eq. (3.18) becomes:

$$U = \lambda\left(\frac{-1 + e^{-\eta\,\mathrm{Re}}}{e^{-\mathrm{Re}} - 1}\right). \tag{3.19}$$

Here we also used some important quantities of surface skin friction, Nusselt number and Sherwood number at both surface which are given as under:

$$\begin{aligned} &Cf_1 = \frac{L^2\tau_1}{\rho\upsilon^2} = e^{-\delta\theta}\frac{dU}{d\eta}\Big|_{\eta=0,1},\quad Cf_2 = \frac{L^2\tau_2}{\rho\upsilon^2} = e^{-\delta\theta}\frac{dW}{d\eta}\Big|_{\eta=0,1},\\ &Nu = \frac{Lq_m}{k(T_1 - T_f)} = -\frac{d\theta}{d\eta}\Big|_{\eta=0,1},\quad Sh = \frac{Lq_w}{D_B(CC_1 - C_0)} = -\frac{d\varphi}{d\eta}\Big|_{\eta=0,1} \end{aligned} \tag{3.20}$$

where

$$\tau_1 = \mu\frac{du}{dy},\ \tau_2 = \mu\frac{dw}{dy},\ q_m = -k\frac{dT}{dy},\ q_w = -D_B\frac{dC}{dy}. \tag{3.21}$$

3.2 Results and Discussion

By using RK-method, MHD Coutte-Poiseuille (CP) flow is numerically inspected with mass & heat transfer in a rotating channel. To check numerical results, we compared these results with exact solutions for some particular cases which are presented in Table 3.1. Hence the results conducted by comparison methods proved that numerical method is more efficient than exact solution.

Figure 3.2(a) and 3.2(b) clearly show the effect of M and viscosity on $U(\eta)$ and $W(\eta)$. $U(\eta)$ increased by increasing the value of both parameters. For larger values of M with δ as shown in Figure 3.2(a) $U(\eta)$ converges very fast. Similarly the same result shows in Figure 3.2(b) for $W(\eta)$. The consequences of the reality, magnetic field is usually reduced the velocity gradient and $W(\eta)$ is zero with the hydrodynamic BC for surface.

Figure 3.3(a) and 3.3(b) describe the influence of m and Re on $U(\eta)$ and $W(\eta)$. In these Figures, due to the presence of m we note that the $U(\eta)$ decreased uniformly and also for larger values of Re it converges rapidly. $U(\eta)$ and $W(\eta)$ decreased by increasing the values of m.

Figure 3.4(a) & 3.4 (b) depict the influence of λ and R_0 on $U(\eta)$ and $W(\eta)$. $U(\eta)$ increased with λ and R_0, whereas its value zero at the bottom. Figure 3.5(a) and 3.5(b) show the effects of R_0, Re, λ & M on the $\theta(\eta)$. The $\theta(\eta)$ increased with λ and R_0, as describes in Figure 3.5(a). Additionally, $\theta(\eta)$ increased for larger values of Re.

In Figures 3.6(a) and 3.6(b) show the influence of Bi and Ec on $\theta(\eta)$ in addition with m and δ. $\theta(\eta)$ decreased for both parameters i.e m and δ.

The impact of magnetic parameters for primary flow on Cf_1 at top and bottom between parallel walls with λ and R_0 are described in Figures 3.7(a) and 3.7(b). Skin friction is examined to be decreased and increased just because of magnetic field. Cf_1 at top surface

changes from bottom surface and with smaller values of R_0, λ as presented in Figure 3.7(b).

The impact of secondary flow in two parallel walls on the bottom surface for Cf_2 with λ, R_0, Re and magnetic parameters are shown in Figure 3.8(a) and 3.8(b). Since in the secondary flow, due to magnetic field and R_0, Cf_2 at lower surface is decreased. Figures 3.9(a) and (b) elucidates the influence of dimensional number and appropriate NF main flow parameters at the top and bottom on Nu. It is also observed that Ec, R_0 and Nu at lower surface decreased with M in Figure 3.9(a) and therefore the heat exchange rate is reduced. Figure 3.9(b) depicts that Nu decreases but for upper surface motion is increased with Ec.

The effects of Sh for primary flow with Le is depicted in Figures 3.10(a) and 3.10(b) at bottom and top. Sh decreases with Nb and Le at both of bottom and top surfaces.

Table 3.1: Comparison of exact and numerical outcomes of $U(\eta)$.

η	Case 1: $\delta = Re = M = Ro = 0$		Case 2: $\delta = Re = m = Ro = 0$		Case 3: $\delta = Ro = M = 0$	
	Numerical	Exact	Numerical	Exact	Numerical	Exact
0	0	0	0	0	0	0
0.1	0.05	0.05	0.0569	0.0570	0.0753	0.0753
0.2	0.10	0.10	0.1115	0.1116	0.1434	0.1433
0.3	0.15	0.15	0.1642	0.1642	0.2050	0.2050
0.4	0.20	0.20	0.2153	0.2153	0.2607	0.2607
0.5	0.25	0.25	0.2649	0.2649	0.3112	0.3113
0.6	0.30	0.30	0.3133	0.3134	0.3568	0.3569
0.7	0.35	0.35	0.3608	0.3606	0.3982	0.3982
0.8	0.40	0.40	0.4076	0.4076	0.4356	0.4357
0.9	0.45	0.45	0.4539	0.4539	0.4694	0.4694
1	0.50	0.50	0.5000	0.4999	0.5000	0.5000

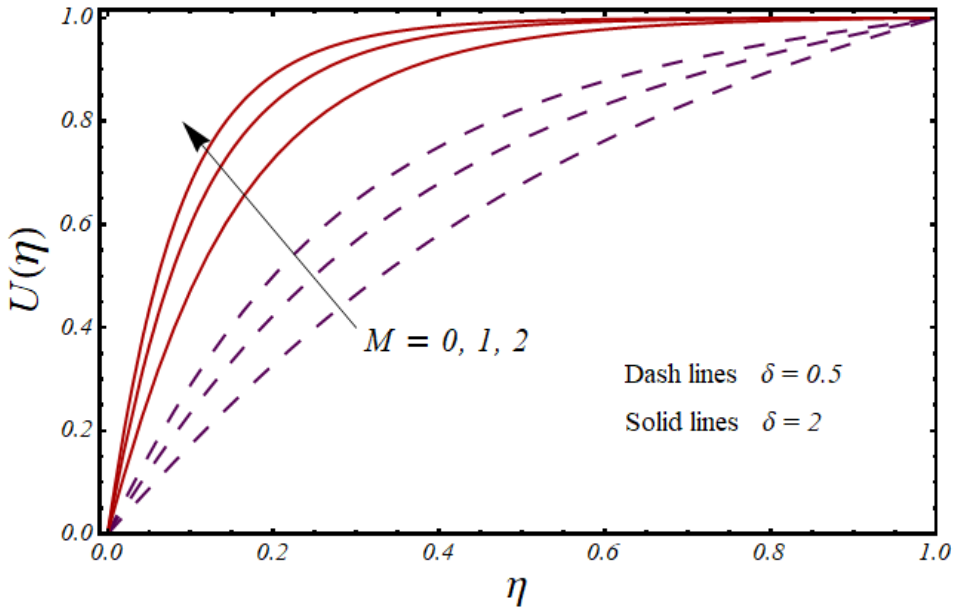

(a)

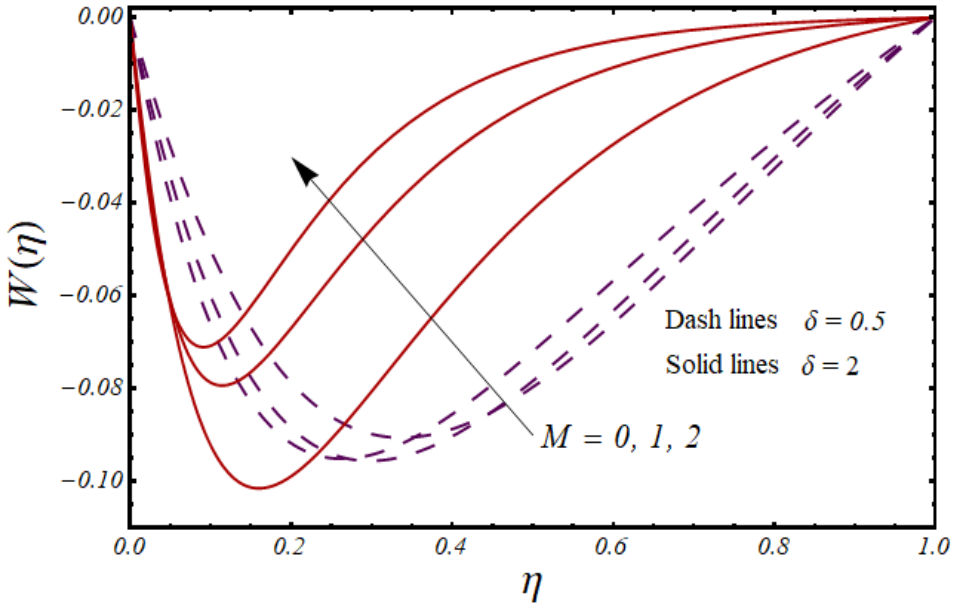

(b)

Figure 3.2: $U(\eta)$ and $W(\eta)$ with M .

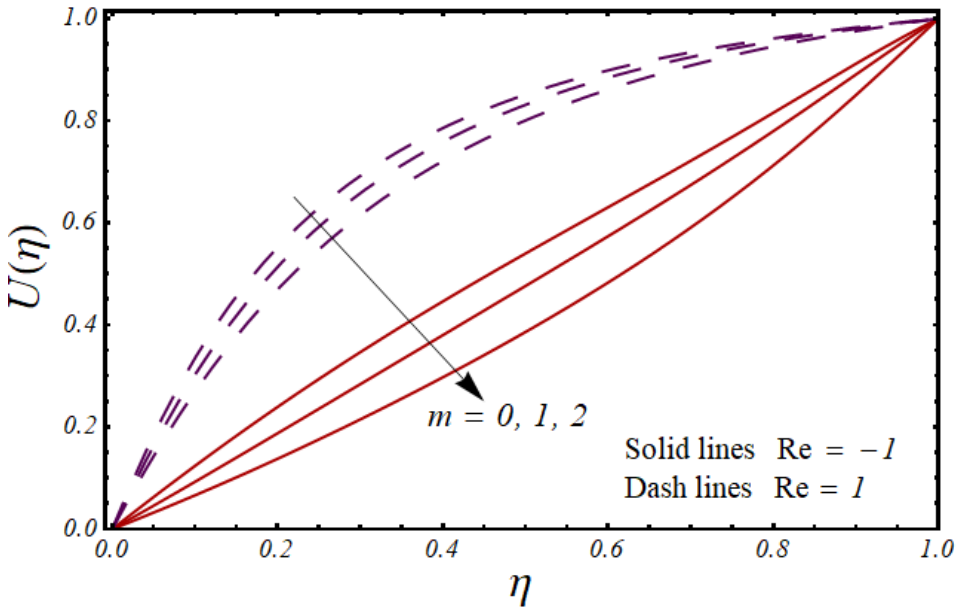

(a)

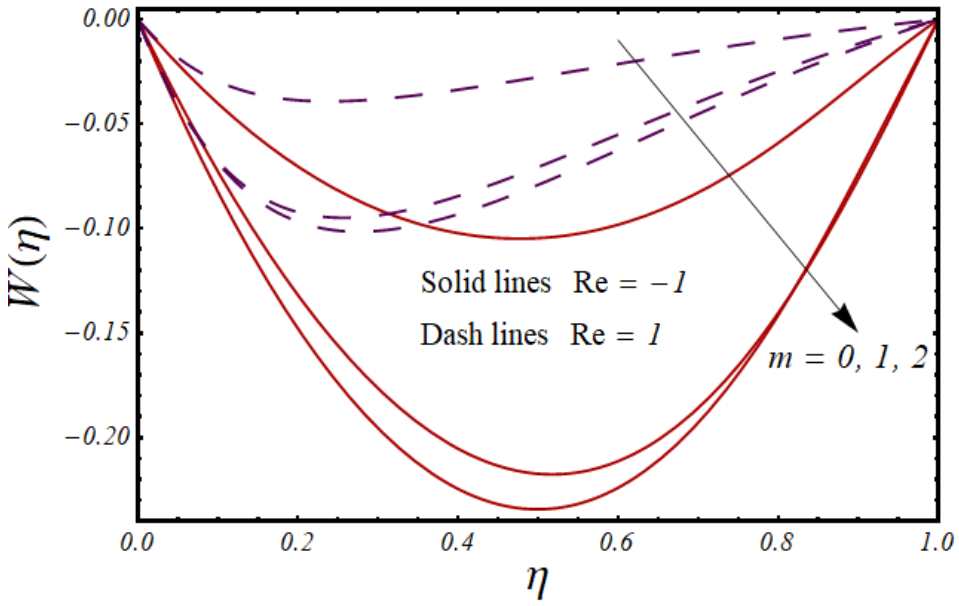

(b)

Figure 3.3: $U(\eta)$ and $W(\eta)$ with m.

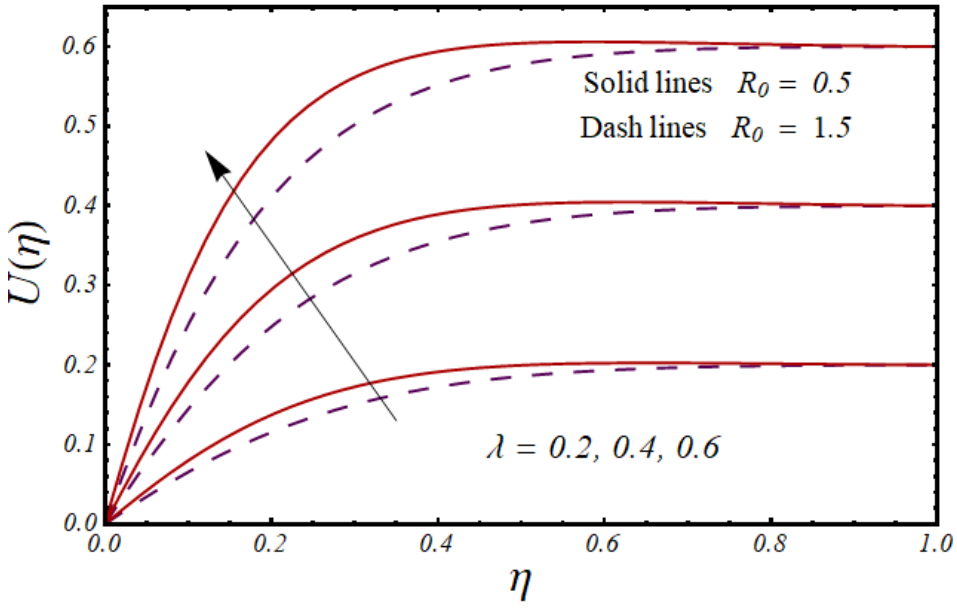

(a)

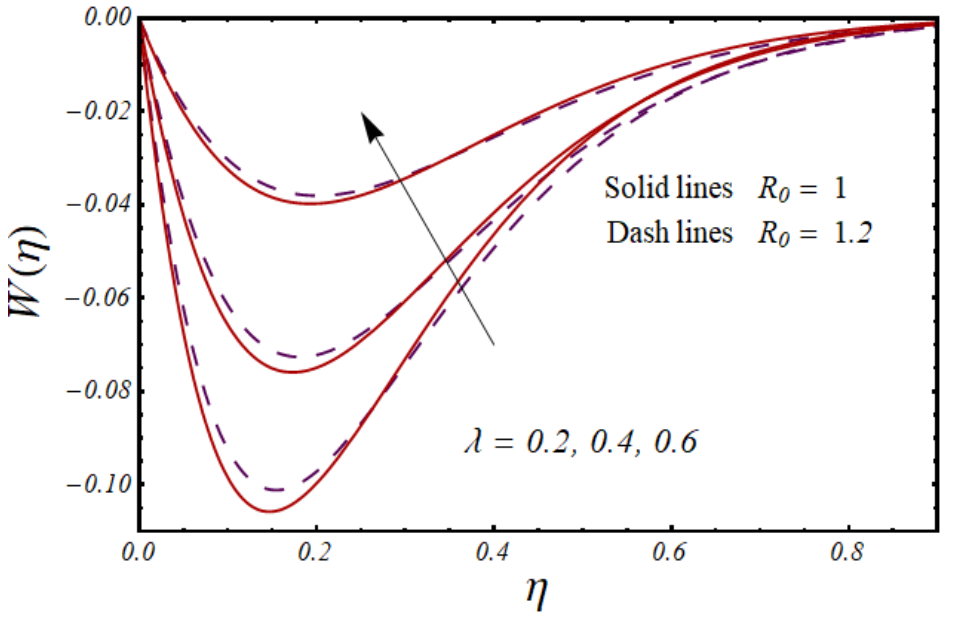

(b)

Figure 3.4: $U(\eta)$ and $W(\eta)$ with λ .

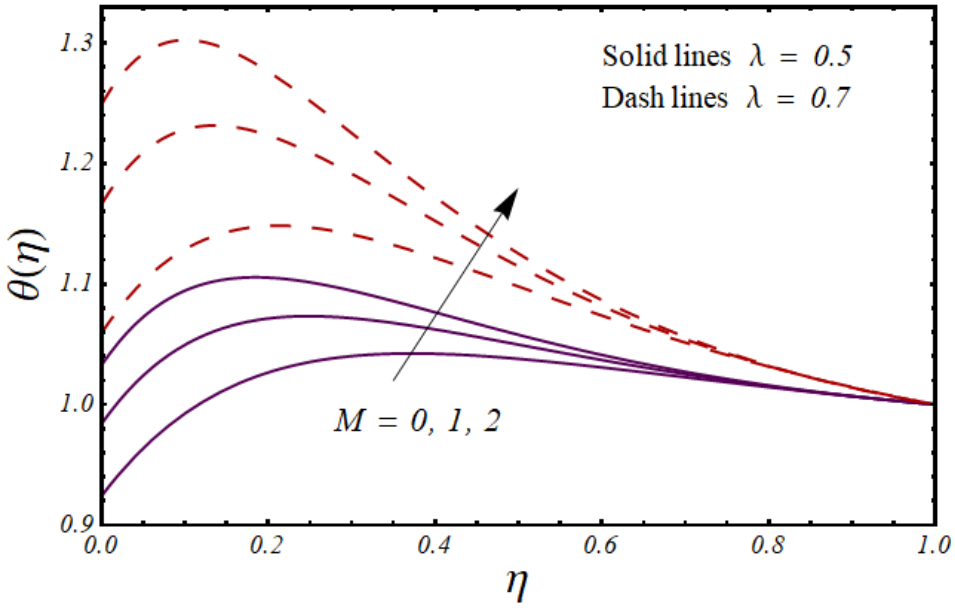

(a)

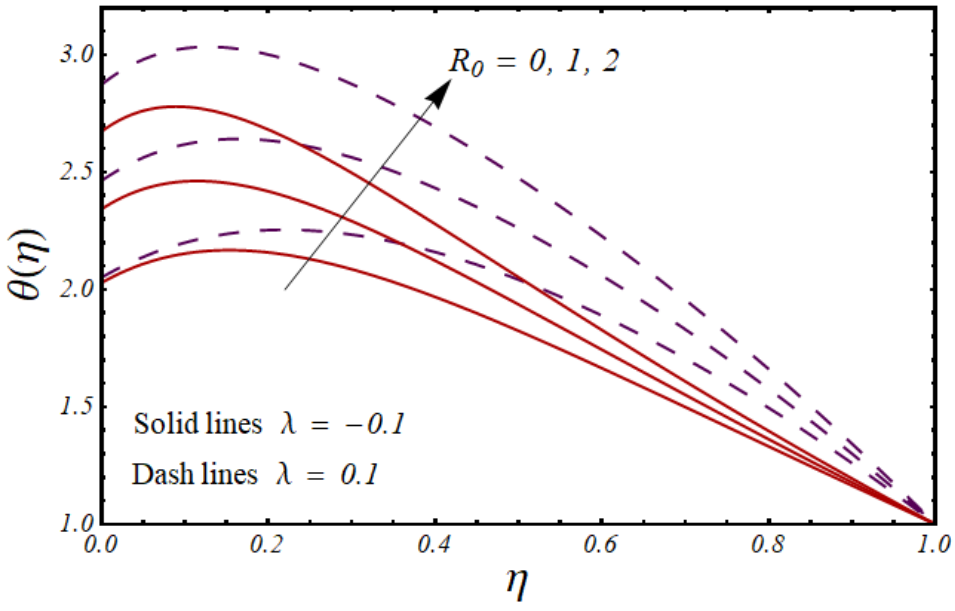

(b)

Figure 3.5: $\theta(\eta)$ with M and R_0.

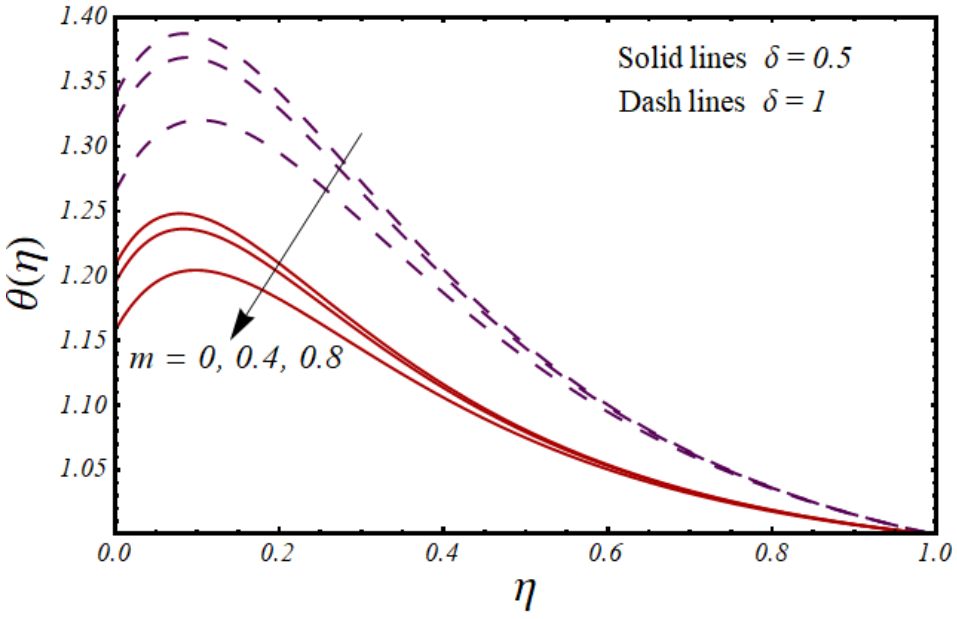

(a)

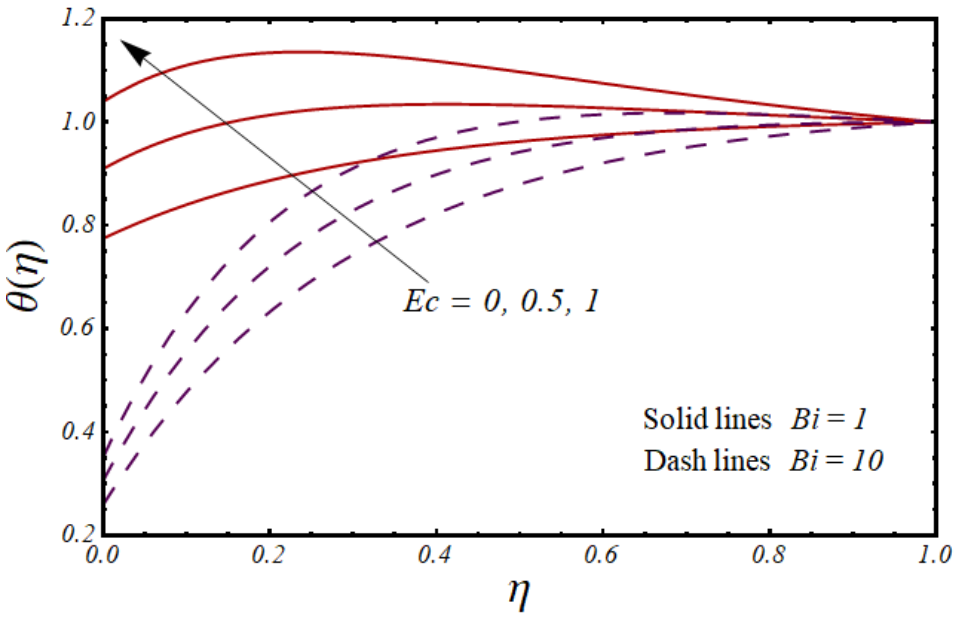

(b)

Figure 3.6: $\theta(\eta)$ with m and Ec.

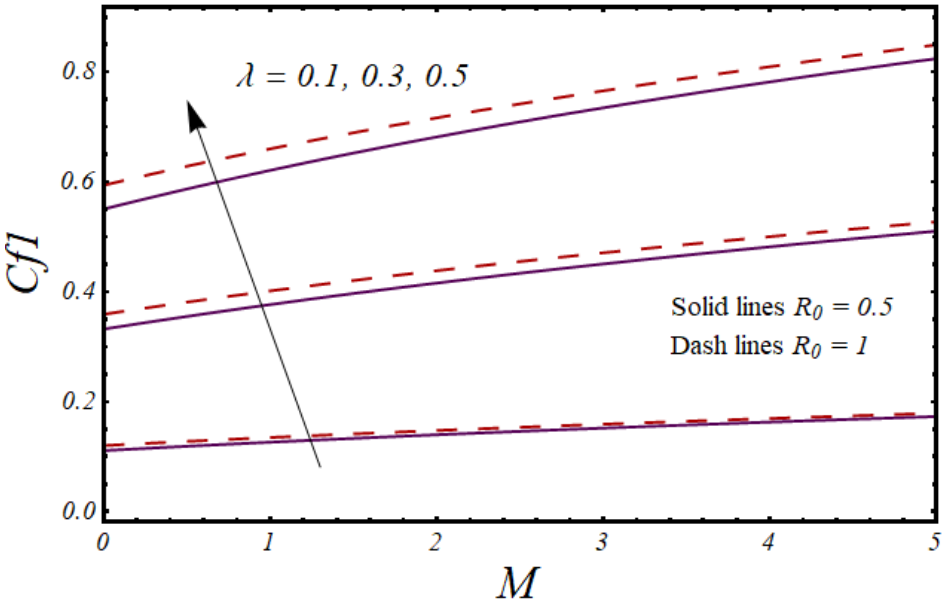

(a)

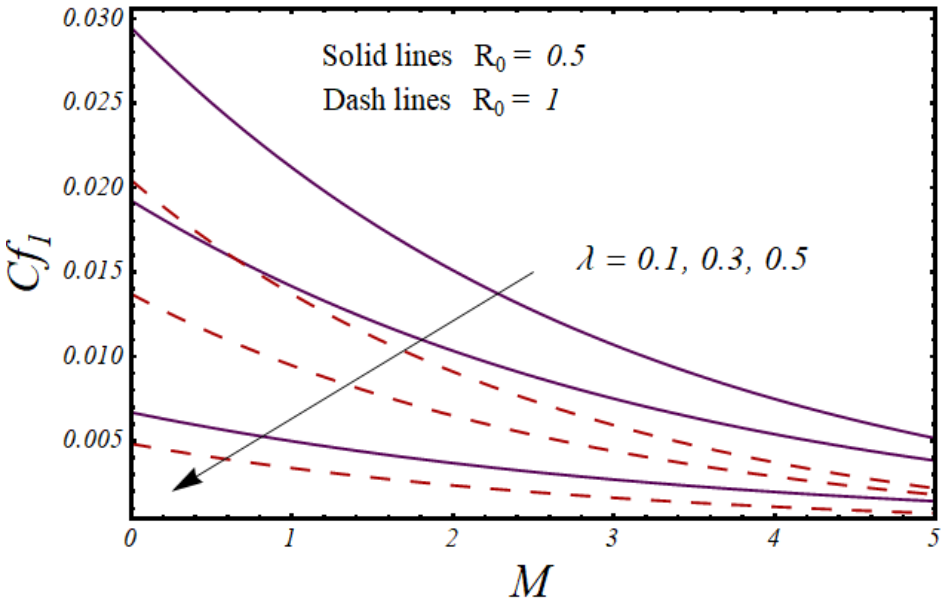

(b)

Figure 3.7: Cf_1 versus λ and R_0.

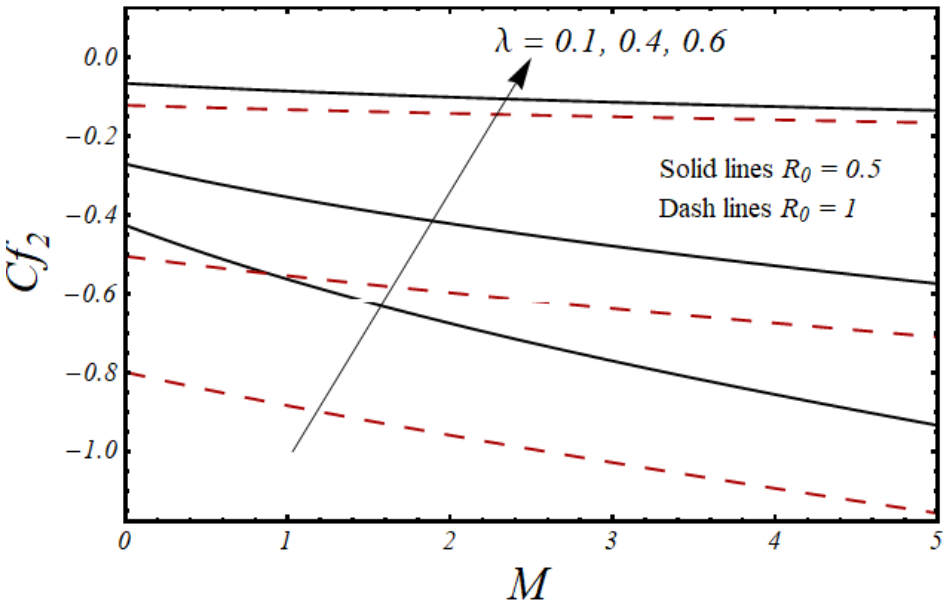

(a)

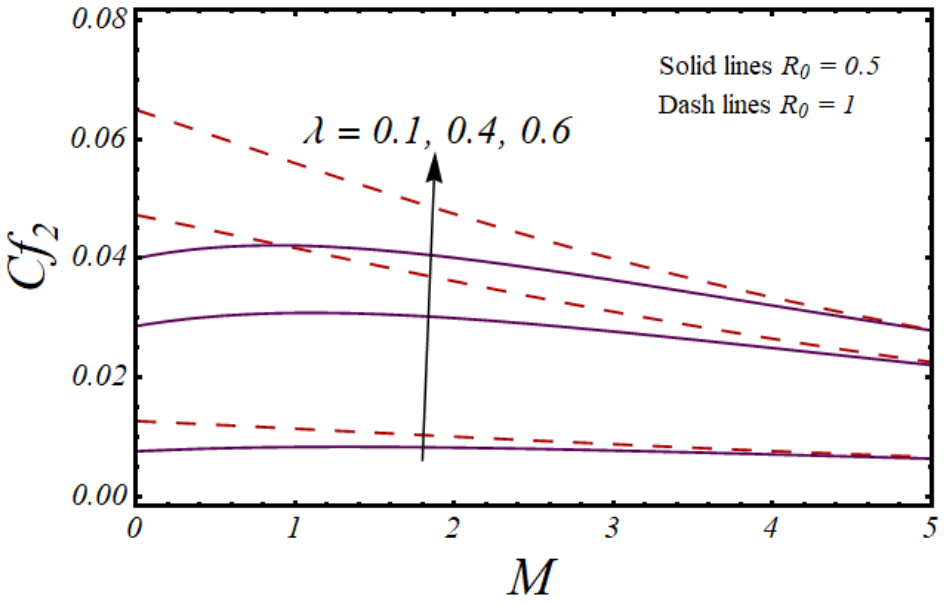

(b)

Figure 3.8: Cf_2 versus λ and R_0.

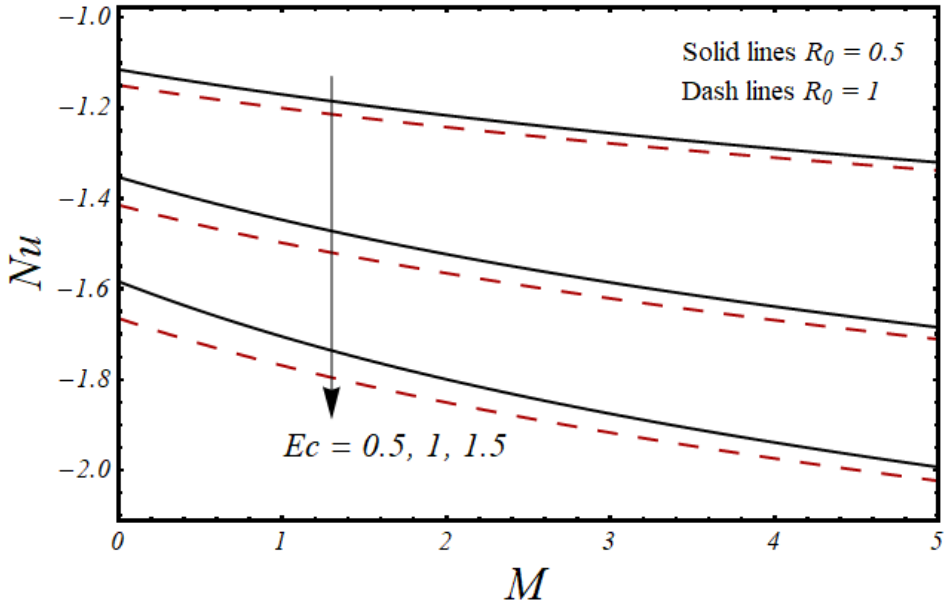

(a)

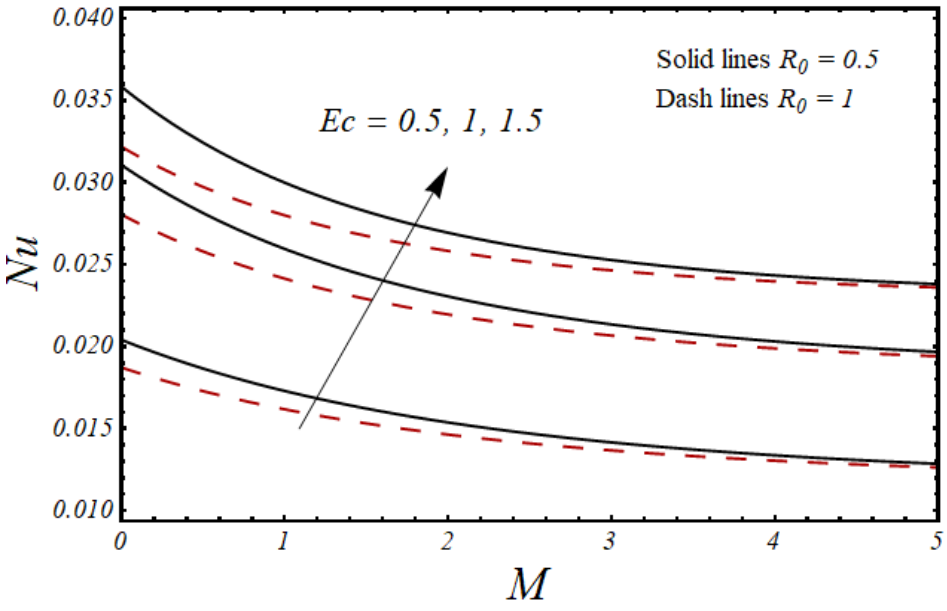

(b)

Figure 3.9: *Nu* with *Ec* and R_0.

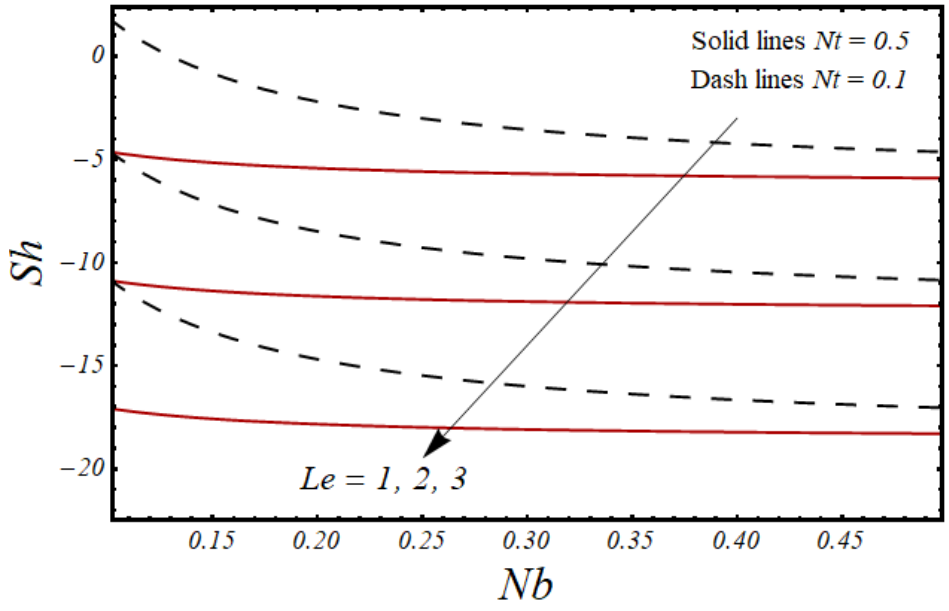

(a)

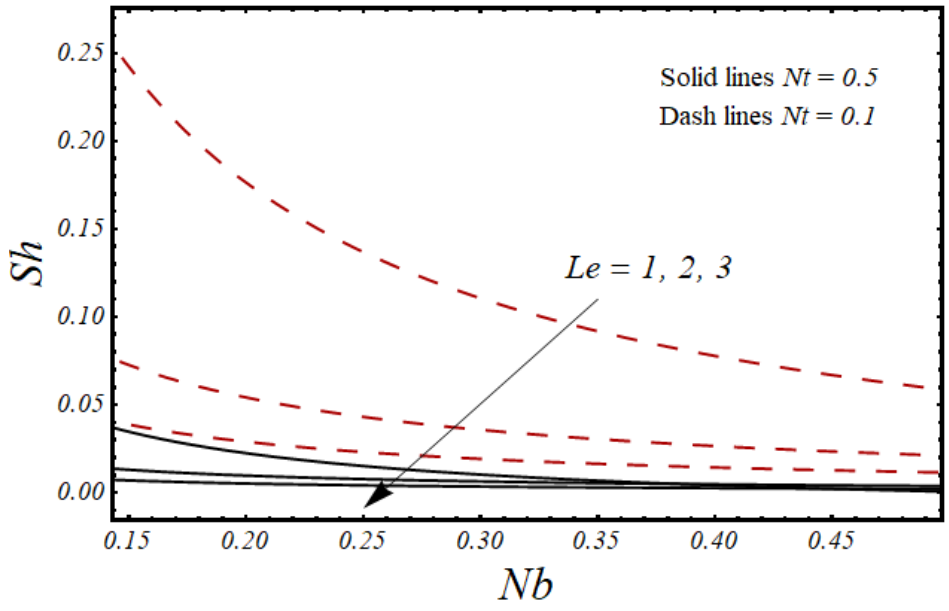

(b)

Figure 3.10: *Sh* with *Le* and *Nt* .

Chapter 4

Study of Couette-Poiseuille flow of kerosene based ferrofluid in a rotating channel with mass transfer and slip effect

4.1 Introduction

This chapter presents an analysis on CP flow of kerosene based nanofluid in a rotating channel. The contribution of wall slip on the flow is examined with magnetic field. Mass transfer analysis is also carried out. In combination with non-linear ODEs, similarity transformation is used to transform the governing equations. For solution of these non-liner ODEs, the same procedure is adopted which applied in previous chapter. Finally, the results are shown via graphs.

4.2 Problem Formulation

Figure 4.1 reflects the geometry of the problem consisting of two infinite plates with temperatures T_1 and T_f while h_f is the heat transfer coefficient. All physical parameters depend on y - axis expect pressure. The channel is filled with kerosene based FF and ferro particles (FP) (Ferrimagnetic cobalt ferrite ($CoFe_2O_4$)). Table 4.1 outlines the NF's thermo-physical characteristics.

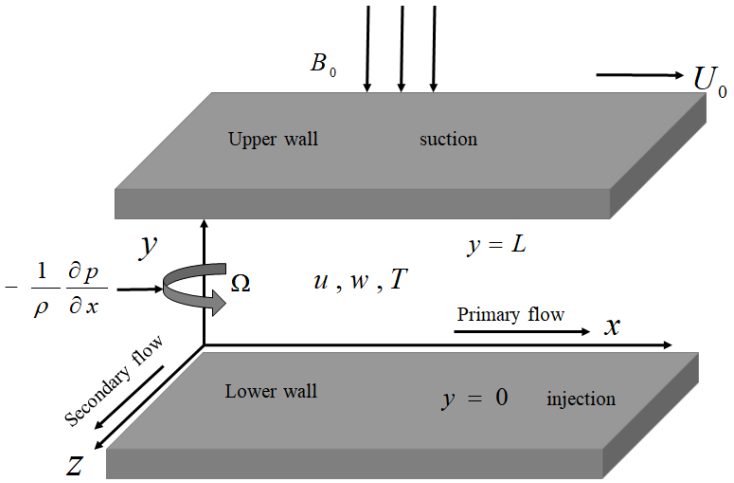

Figure 4.1: Physical configuration of the problem

The equations for flow fluid, under the above suppositions are as follows

$$-V\frac{du}{dy}+2\Omega w=\frac{1}{\rho_{nf}}\frac{d}{dy}\left(\mu_{nf}\frac{du}{dy}\right)-\frac{\sigma_{nf}B_0^{\,2}\left(u-U_0+mw\right)}{\rho_{nf}\left(1+m^2\right)}, \tag{4.1}$$

$$-V\frac{dw}{dy}-2\Omega\left(u-U_0\right)=\frac{1}{\rho_{nf}}\frac{d}{dy}\left(\mu_{nf}\frac{dw}{dy}\right)-\frac{\sigma_{nf}B_0^{\,2}\left(w-mu+mU_0\right)}{\rho_{nf}\left(1+m^2\right)}, \tag{4.2}$$

$$-V\frac{dT}{dy}=\alpha_{nf}\frac{d^2T}{dy^2}+\frac{\mu_{nf}}{(\rho c_p)_{nf}}\left(\left(\frac{du}{dy}\right)^2+\left(\frac{dw}{dy}\right)^2\right)+\frac{\sigma_{nf}B_0^{\,2}}{\left(\rho c_p\right)_{nf}}\left(\frac{(u-U_0+mu)^2+(w-mu+mU_0)^2}{\left(1+m^2\right)^2}\right), \tag{4.3}$$

$$-V\frac{dC}{dy}=D\frac{d^2C}{dy^2}-k_n\left(C_1-C_0\right)^n. \tag{4.4}$$

$$\mu_{nf}=\frac{\mu_f}{\left(1-\varphi\right)^{2.5}},\alpha_{nf}=\frac{\kappa_{nf}}{\left(\rho C_p\right)_{nf}},\quad \rho_{nf}=\varphi\rho_s+\left(1-\varphi\right)\rho_f,$$
$$\frac{\kappa_{nf}}{\kappa_f}=\frac{\kappa_s+(\mathrm{n}_p-1)\kappa_f-(\mathrm{n}_p-1)\varphi\left(\kappa_f-\kappa_s\right)}{\kappa_s+(\mathrm{n}_p-1)\kappa_f+\varphi\left(\kappa_f-\kappa_s\right)},\left(\rho C_p\right)_{nf}=\left(1-\varphi\right)\left(\rho C_p\right)_f+\varphi\left(\rho C_p\right)_s. \tag{4.5}$$

Here $n_p=3$ for spherical shaped and $n_p=1.5$ for cylindrical shaped [42].

Table 4.1 Thermo physical quantities of ferroparticle and kerosene oil [42].

Liquid/ NPs	ρ (kg/m^3)	C_p (J/kg K)	κ (W/m K)
Kerosene oil	783	2090	0.15
$CoFe_2O_4$	4907	700	3.7

The appropriate BCs of the present problem are

$$u = b_1 \frac{du}{dy},\ w = b_1 \frac{dw}{dy},\ C = C_0,\ -k\frac{dT}{dy} = h_f (T_f - T),\ \text{at } y = 0,$$
$$u = U_0,\ C = C_1,\ T = T_1,\ w = 0 \text{ at } y = L. \tag{4.6}$$

Here b_1 is the velocity slip length.

By using equation (3.7) and the following dimensionless quantities

$$\mathrm{Sc} = \frac{L\upsilon}{D},\ \gamma = k_n \frac{L}{\upsilon}\left(C_1 - C_0\right)^{n-1},\ \alpha = b_1 \frac{\upsilon_f}{L^2}, \tag{4.7}$$

Eqs. (4.1)-(4.7) become

$$-Re\frac{dU}{d\eta} + 2RoW = \frac{1}{A_1 A_2}\left(-\delta e^{-\delta\theta}\frac{d\theta}{d\eta}\frac{dU}{d\eta} + e^{-\delta\theta}\frac{d^2U}{d\eta^2}\right) - \frac{1}{A_1}\left(\frac{M\left(mW + U - \lambda\right)}{\left(m^2+1\right)}\right), \tag{4.8}$$

$$\text{-}Re\frac{dU}{d\eta} - 2Ro\left(U - \lambda\right) = \frac{1}{A_1 A_2}\left(e^{-\delta\theta}\frac{d^2W}{d\eta^2} - \delta e^{-\delta\theta}\frac{d\theta}{d\eta}\frac{dU}{d\eta}\right) - \frac{1}{A_1}\left(\frac{M\left(W - mU + m\lambda\right)}{\left(1+m^2\right)}\right), \tag{4.9}$$

$$A_4\frac{d^2\theta}{d\eta^2} + A_3\,\mathrm{Re}\,\mathrm{Pr}\frac{d\theta}{d\eta} + \frac{1}{A_1}\left(Ec\left(\left(\frac{dU}{d\eta}\right)^2 + \left(\frac{dW}{d\eta}\right)^2\right)\mathrm{Pr}\,e^{-\delta\theta}\right) + Ec\,\mathrm{Pr}\,M\left(\frac{\left(mW + U - \lambda\right)^2 + \left(-mU + m\lambda + W\right)^2}{\left(1+m^2\right)^2}\right) = 0, \tag{4.10}$$

$$\frac{d^2}{d\eta^2}(\phi) + Sc\left(\frac{d}{d\eta}(\phi)\right)\mathrm{Re} - \gamma\left(\frac{d}{d\eta}(\phi)\right)^n Sc = 0, \tag{4.11}$$

where

$$A_1 = \varphi\frac{\rho_s}{\rho_f} + \left(-\varphi + 1\right),\ A_2 = \left(1-\varphi\right)^{2.5},\ \mathrm{A}_3 = \varphi\left(\rho C_p\right)_s\left(\frac{1}{\left(\rho C_p\right)_f}\right) + \left(1-\varphi\right),$$
$$A_4 = \kappa_{nf}\left(\frac{1}{\kappa_f}\right) = \frac{\kappa_s + (\mathrm{n}_p - 1)\kappa_f - \varphi\left(\kappa_f - \kappa_s\right)(\mathrm{n}_p - 1)}{\kappa_s + (\mathrm{n}_p - 1)\kappa_f + \varphi\left(\kappa_f - \kappa_s\right)}.$$

The BCs in new variables become

$$U(0) = \alpha\frac{dU}{d\eta}(0),\ \ W(0) = \alpha\frac{dW}{d\eta}(0),\ \ \frac{d\theta}{d\eta}(0) = Bi\theta(0),\ \ \phi(0) = 0,$$
$$U(1) = \lambda,\ \ W(1) = 0,\ \ \theta(1) = 1,\ \ \phi(1) = 1. \tag{4.12}$$

4.2 Results and Discussion

The above mentioned governing equations (4.8)-(4.11) are solved with BCs at equation (3.12). Figure 4.2 explaines the influence of Re and M on $\mathrm{U}(\eta)$ and $\mathrm{W}(\eta)$ of fluid in a channel with the slip condition. From Figures 4.2(a)-4.2(b) we conclude that velocity increased by rising the values of Re, M and α on lower wall.

The variation of slip parameter on fluid velocities $\mathrm{U}(\eta)$ and $\mathrm{W}(\eta)$ in the whole channel for different values of $m,\ \lambda,\ R_0$ and δ are expressed in Figures 4.3 - 4.4. Figure. 4.3(a)-4.3(b) show the effect on $\mathrm{W}(\eta)$ and $\mathrm{U}(\eta)$ for various values of δ and λ with α. From these Figures, fluid velocity is increased by the increasing values of α. However, an increment in velocity profile is found by increasing the values of λ and δ. Figure. 4.4(a) and 4.4(b) elucidate the effect of Hall and rotation parameters on primary and secondary velocities for zero and non-zero values of slip parameter. We can be observed the varying behavior of α from figures and examined a rapid growth in primary & secondary fluid velocities.

The variation of $\theta(\eta)$ with $\lambda,\ \delta,\ Ec,\ Bi,\ Re$ and R_0 is shown in Figures 4.5-4.7. It can be seen that in Figure 4.5, $\theta(\eta)$ increased with greater values of λ and δ. Furthermore, Figure 4.6 demonstrates that temperature is decreased by Bi, however it increased by Ec. Similarly, $\theta(\eta)$ is increased with R_0, whereas it is increased more with Re which is depicted in Figure 4.7. The curves shown in Figures 4.8 to 4.10 illustrate the diversity in $U(\eta), W(\eta) \& \theta(\eta)$ with the escalating values of φ. From these figures it can be seen that values of $U(\eta), W(\eta)$ and $\theta(\eta)$ increased by increasing the values of φ along with Re and its decreased for smaller values of φ with Re.

In order to examine that how Sc and Re effect $\phi(\eta)$, Figure 4.11 is presented. The value of $\phi(\eta)$ increased gradually by increasing the values of Sc and Re. Since Sc relay inversely with the mass diffusion rate, $\phi(\eta)$ decreased by increasing the Sc. Figure 4.12 depicts the alternation in $\phi(\eta)$ with dissimilar number of Sc and γ. We may conclude from

this figure that for greater values of γ and Sc there is an immense decrease in $\phi(\eta)$ and increase in the concentration with a decrease of both parameters. An increment in $\phi(\eta)$ can be clearly observed with rise in order shape factor n of the chemical reaction and Sc parameter which is presented in Figure 4.13.

Figure 4.14 is plotted to show the effects on skin friction with variation in α and R_0 for primary flow at lower & upper surfaces. This Figure shows that by the increasing the values of α, skin friction is decreased at the lower wall. Figures 4.15(a) and 4.15(b) are presented to show the effects on skin friction with λ on primary velocity due to slip parameter of fluid at the bottom surface and top wall. With an increase α and reduction in R_0, it is concluded that for primary flow the λ and α decreased the Cf_1 for both bottom and top surfaces.

Figure 4.16 is presented to show the variation on Cf_2 for primary flow with R_0 and α at lower & upper surfaces respectively through rotating channel. The Cf_2 is increased by increasing the values of R_0 while an escalation is found averse to α. The variation of Cf_2 with λ and α for secondary flow at both surface is presented in Figure 4.17, in this regard, the secondary flow is noted, λ and M reduced the skin friction for top and bottom surfaces respectively.

The influence of M, R_0 and δ on Nu for primary flow of FF for surfaces is shown in Figure 4.18. It can be found that by increasing the valued of δ, it decreases Nu. Figure 4.19 exhibits the effects on Sh with Sc and γ for primary flow at both surfaces respectively. The Figure show that an increment in Sc will increase Sh, however rise in γ implies the minor decrease in Sh for both surfaces. Figure 4.20(a) and 4.20(b) depict the influence on Sh with various values of Sc and Re. These Figure shows that for primary flow, for the greater values of Re, Sh increased at both lower and upper surfaces.

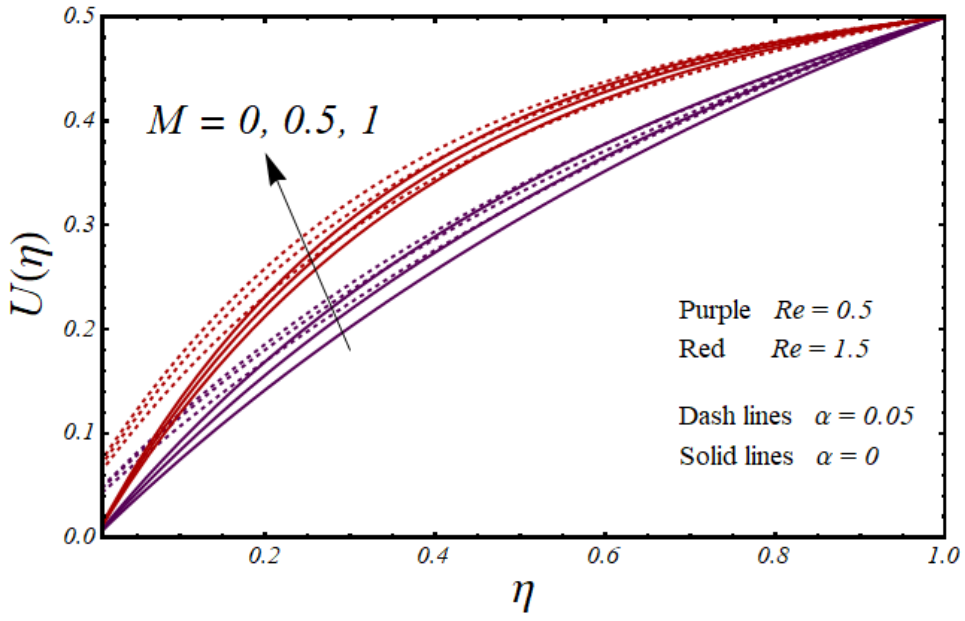

(a)

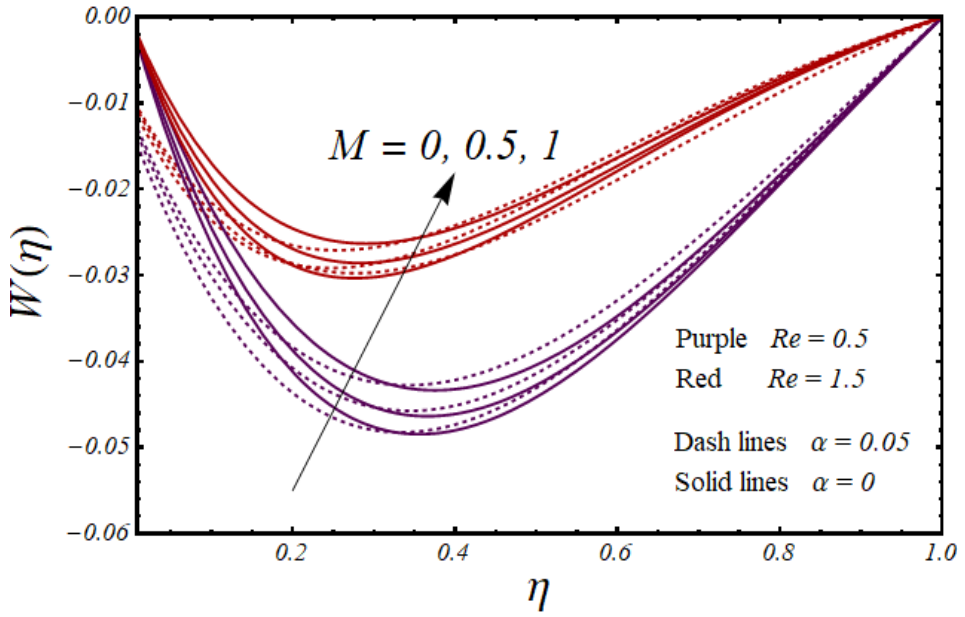

(b)

Figure 4.2: $U(\eta)$ and $W(\eta)$ with Re and α.

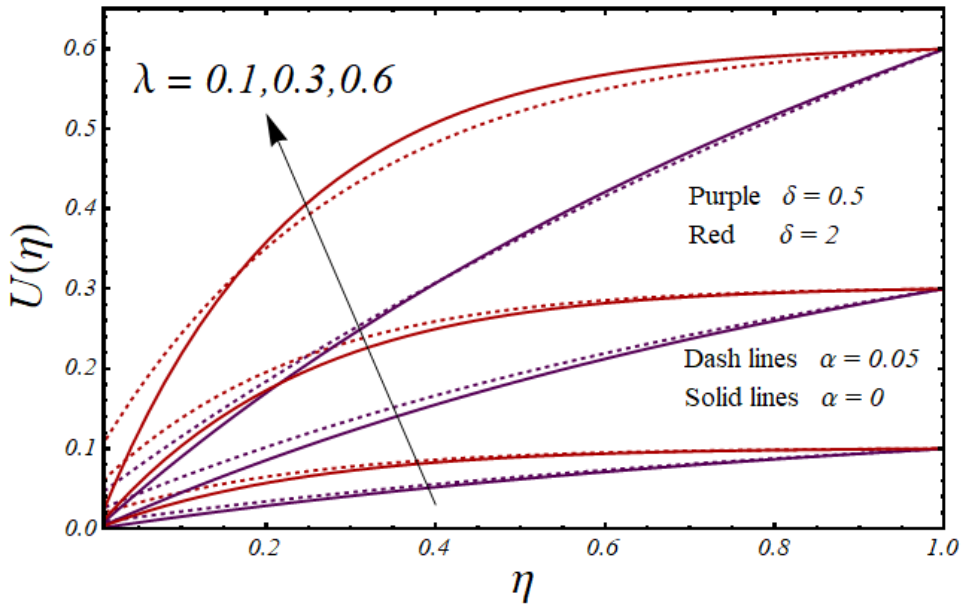

(a)

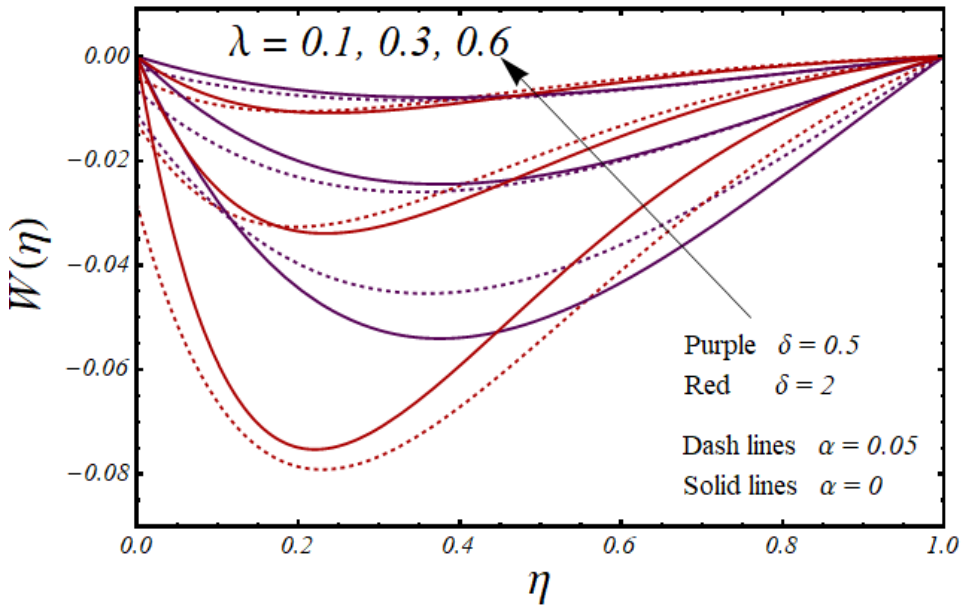

(b)

Figure 4.3: $U(\eta)$ and $W(\eta)$ with λ and α.

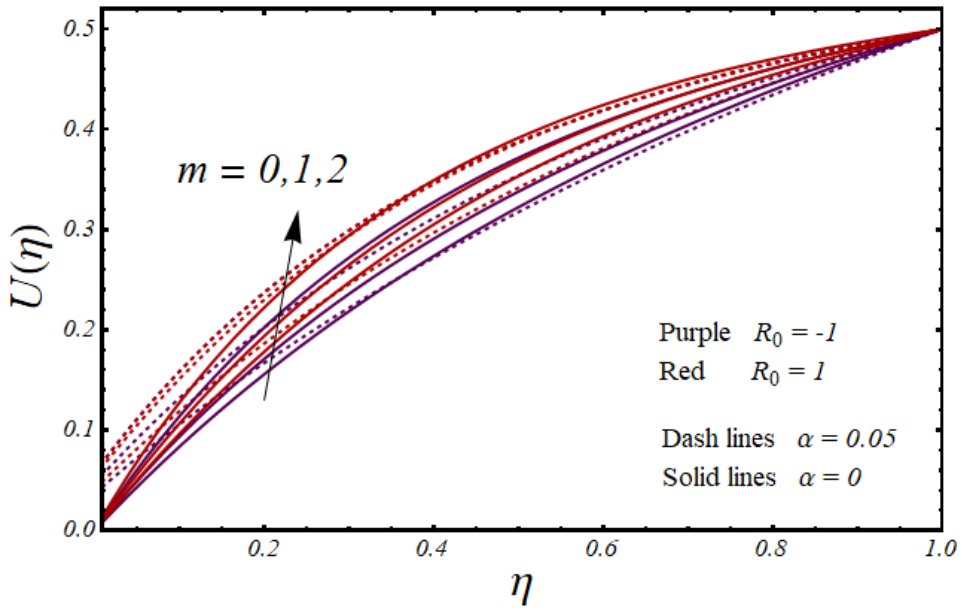

(a)

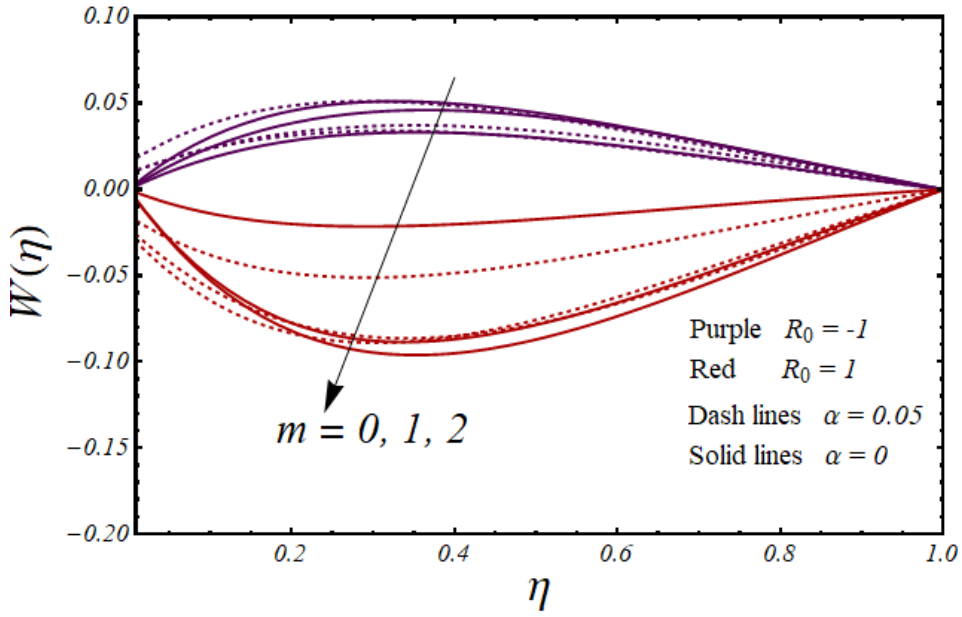

(b)

Figure 4.4: $U(\eta)$ and $W(\eta)$ with m and α.

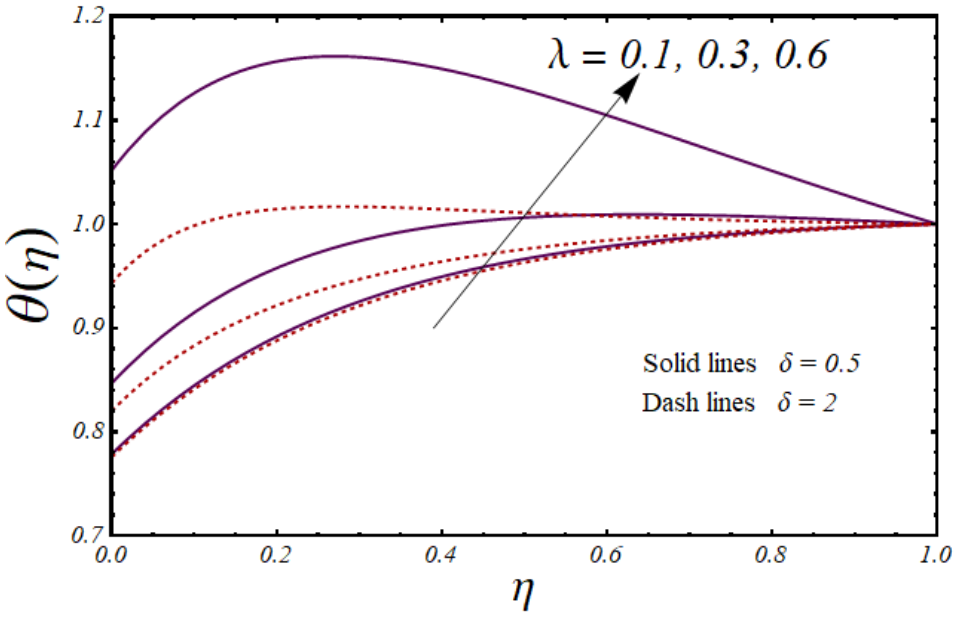

Figure 4.5: $\theta(\eta)$ with λ and δ.

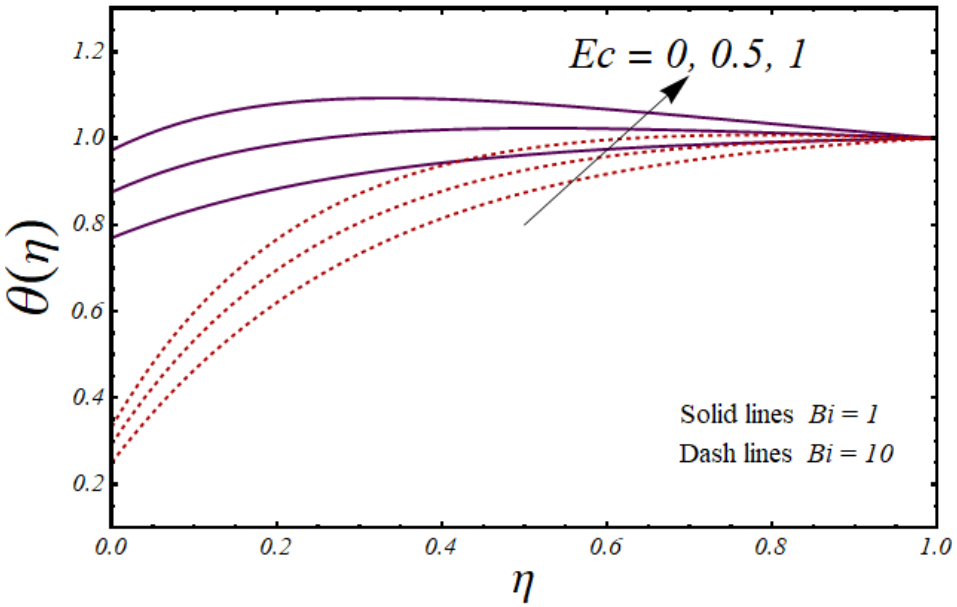

Figure 4.6: $\theta(\eta)$ with Ec and Bi.

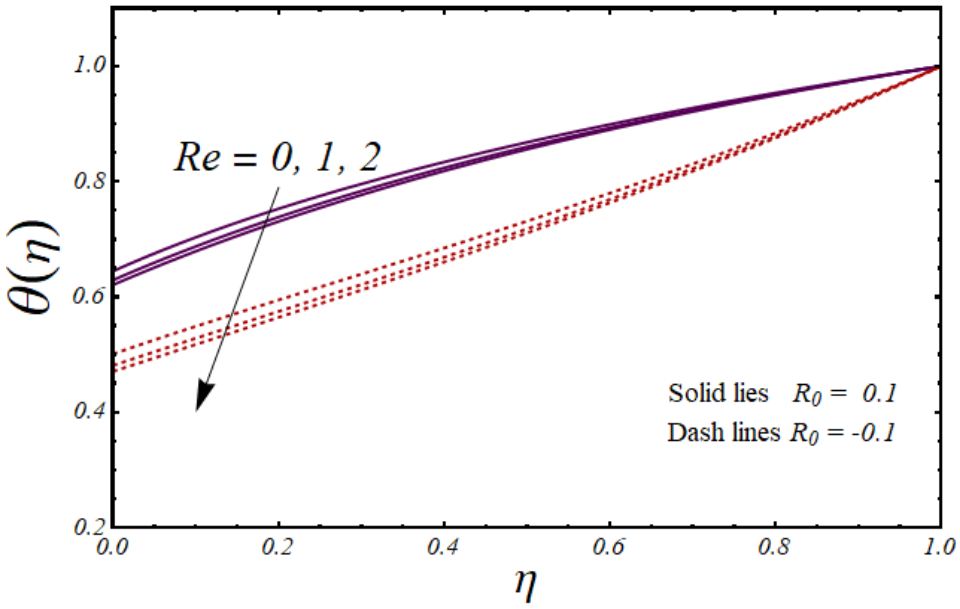

Figure 4.7: $\theta(\eta)$ with Re and R_0.

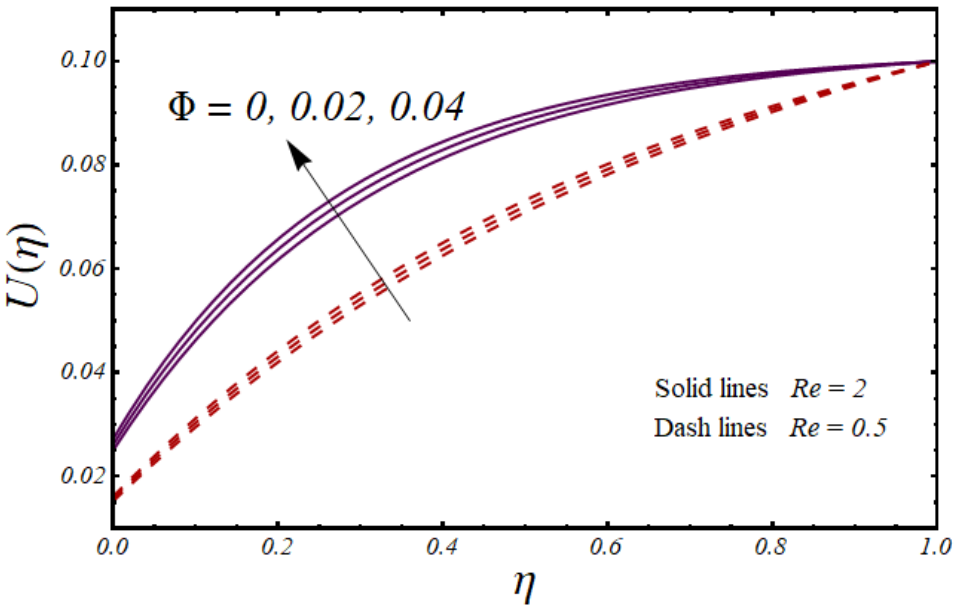

Figure 4.8: $U(\eta)$ with φ and Re.

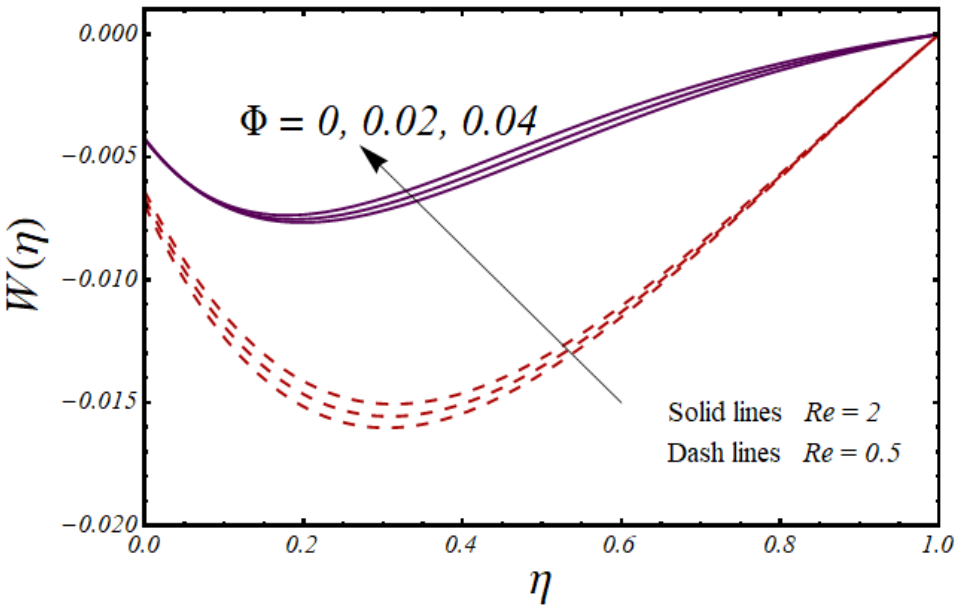

Figure 4.9: $W(\eta)$ with φ and Re .

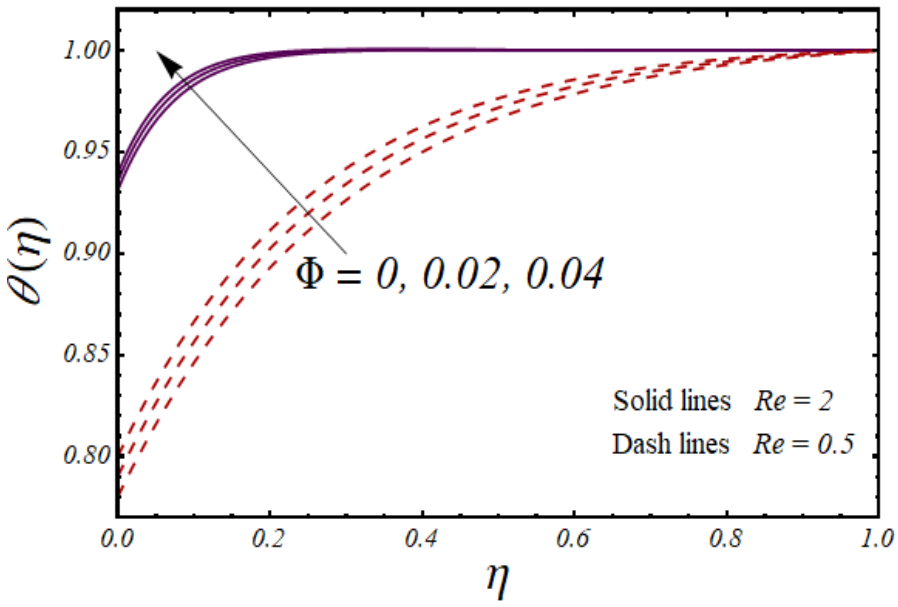

Figure 4.10: $\theta(\eta)$ with φ and Re .

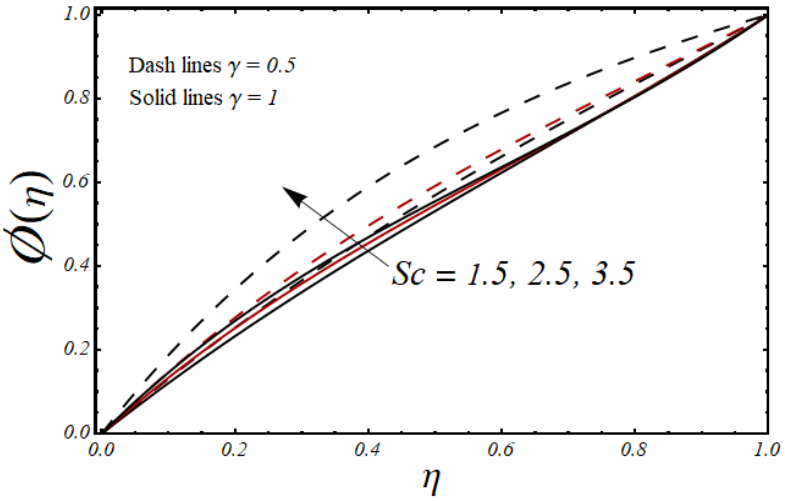

Figure 4.11: $\phi(\eta)$ with Sc and γ.

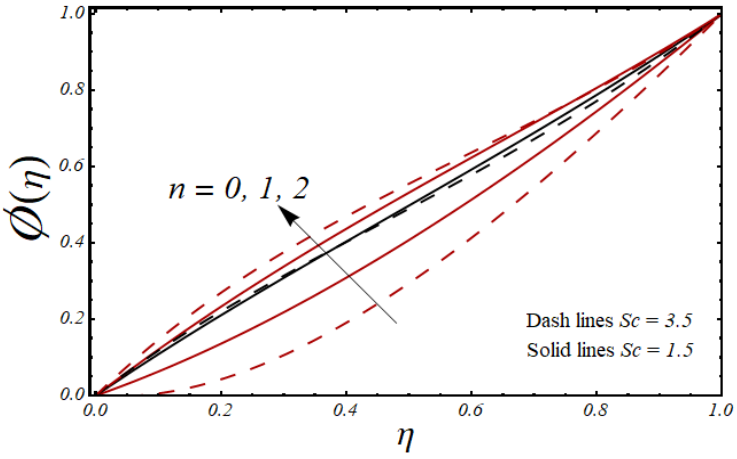

Figure 4.12: $\phi(\eta)$ with n and Sc.

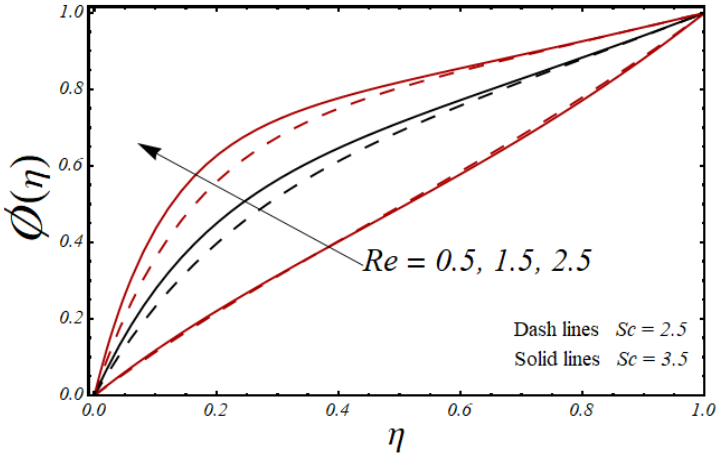

Figure 4.13: $\phi(\eta)$ with Re and Sc.

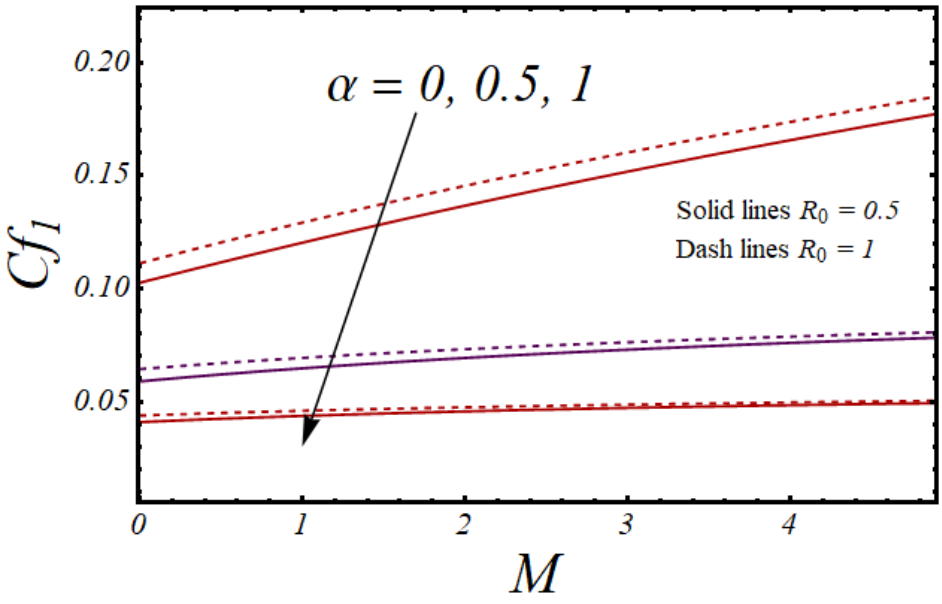

(a)

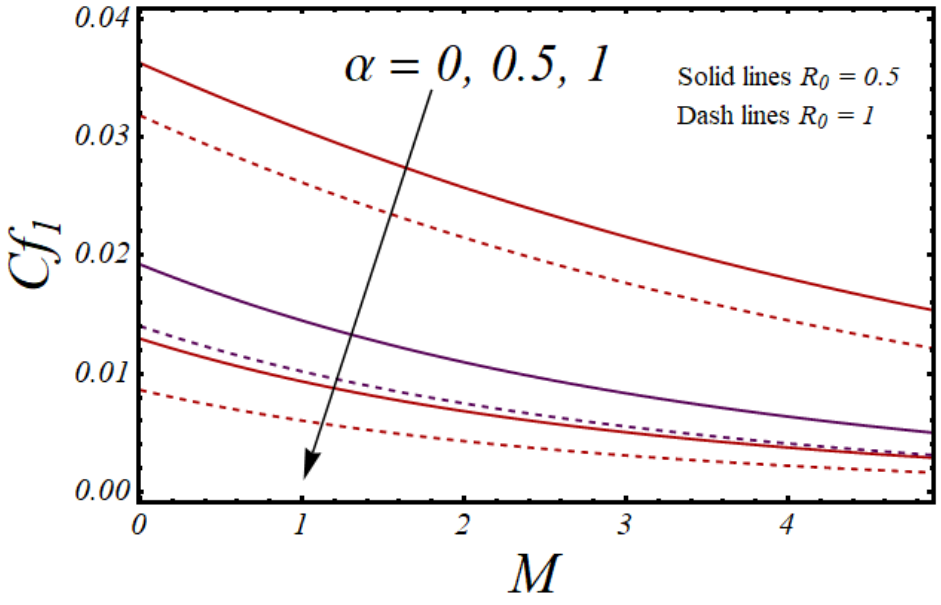

(b)

Figure 4.14: Cf_1 verses α and R_0.

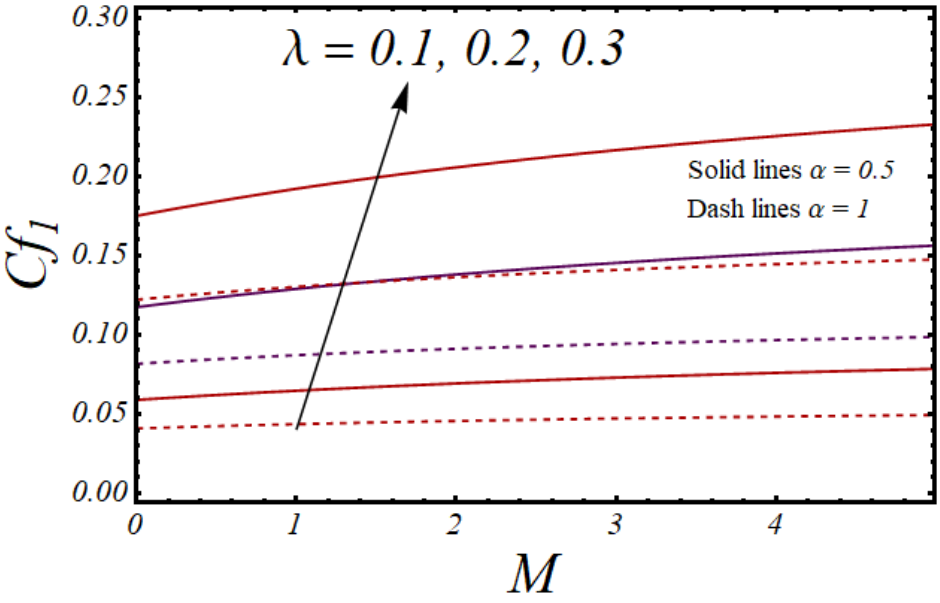

(a)

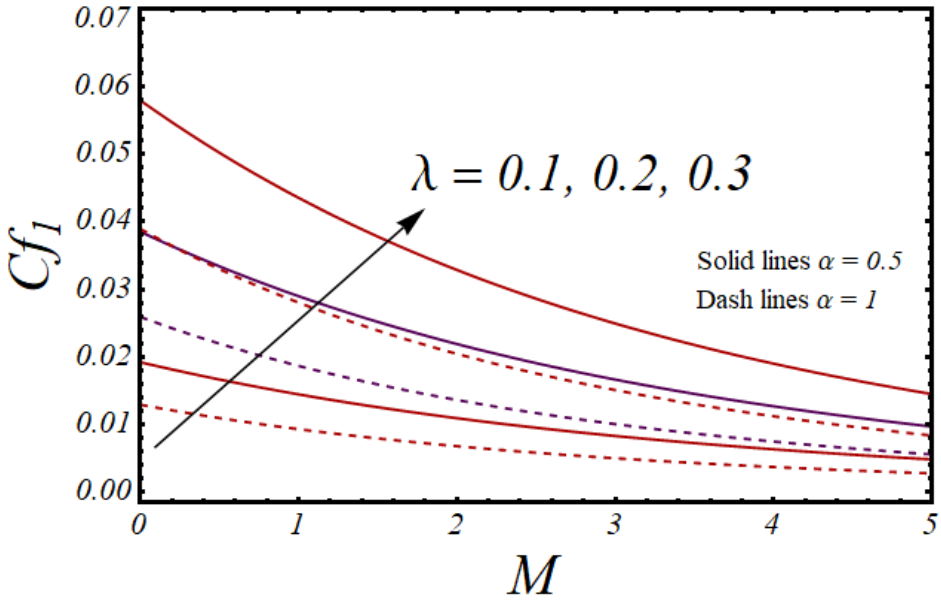

(b)

Figure 4.15: Cf_1 verses λ and α.

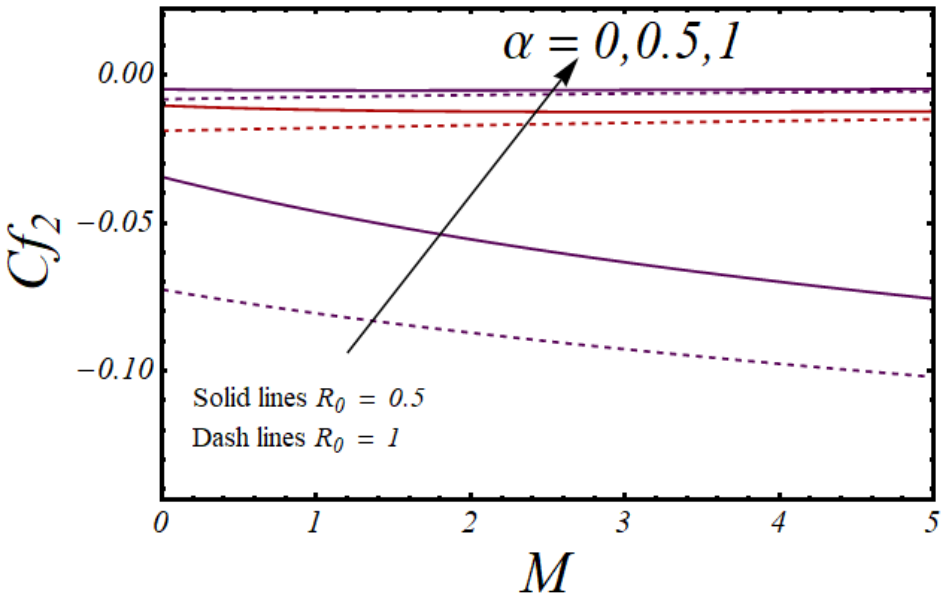

(a)

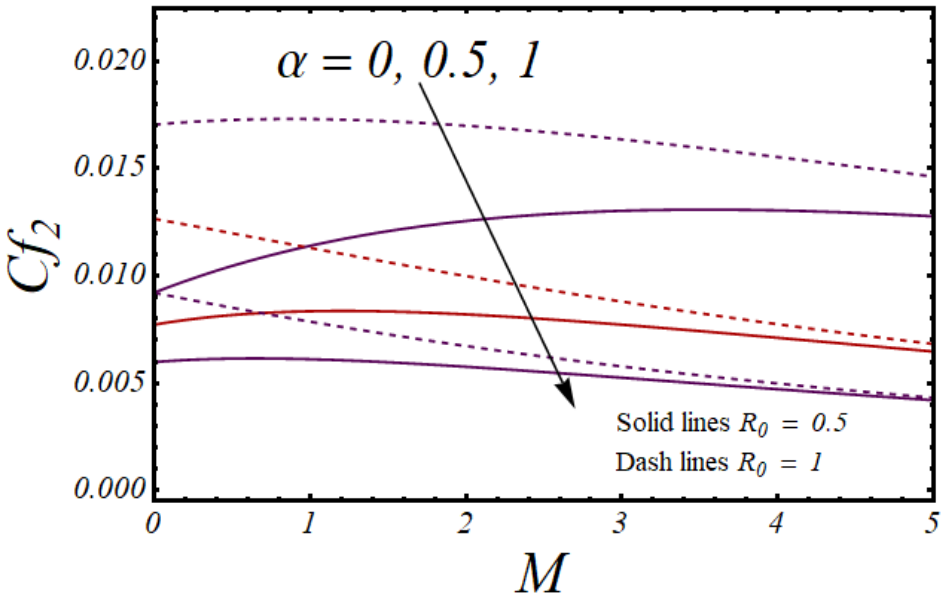

(b)

Figure 4.16: Cf_2 verses α and R_0.

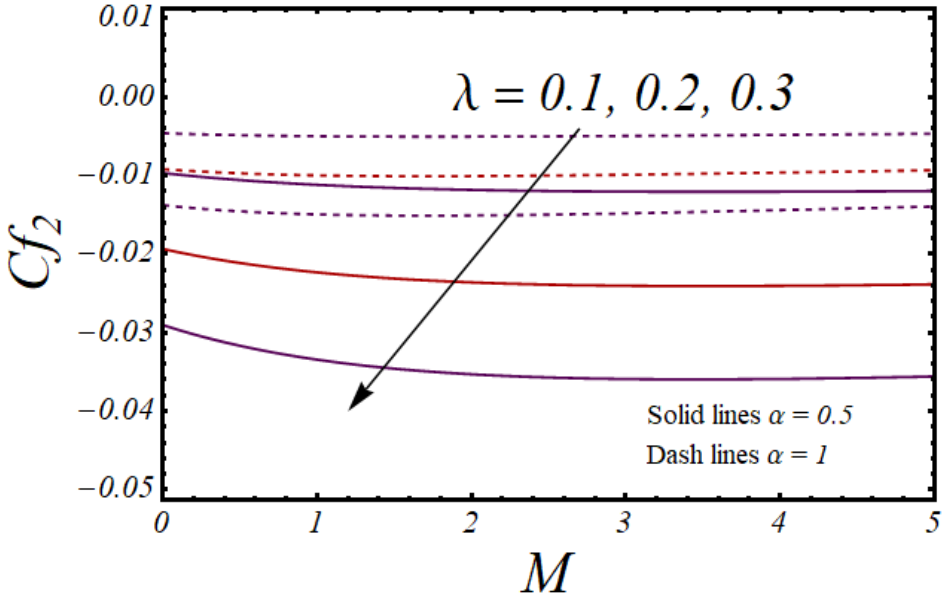

(a)

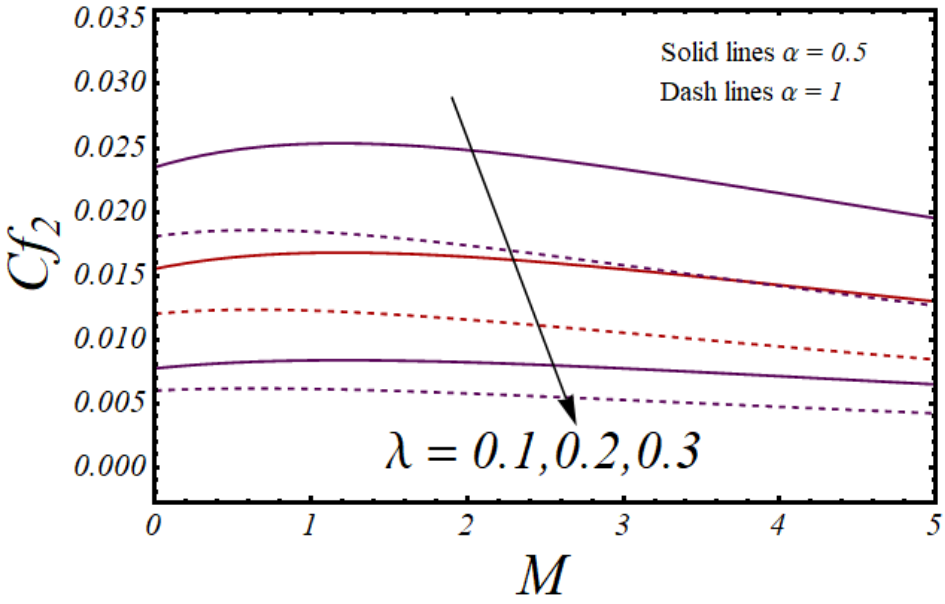

(b)

Figure 4.17: Cf_2 verses with λ and α .

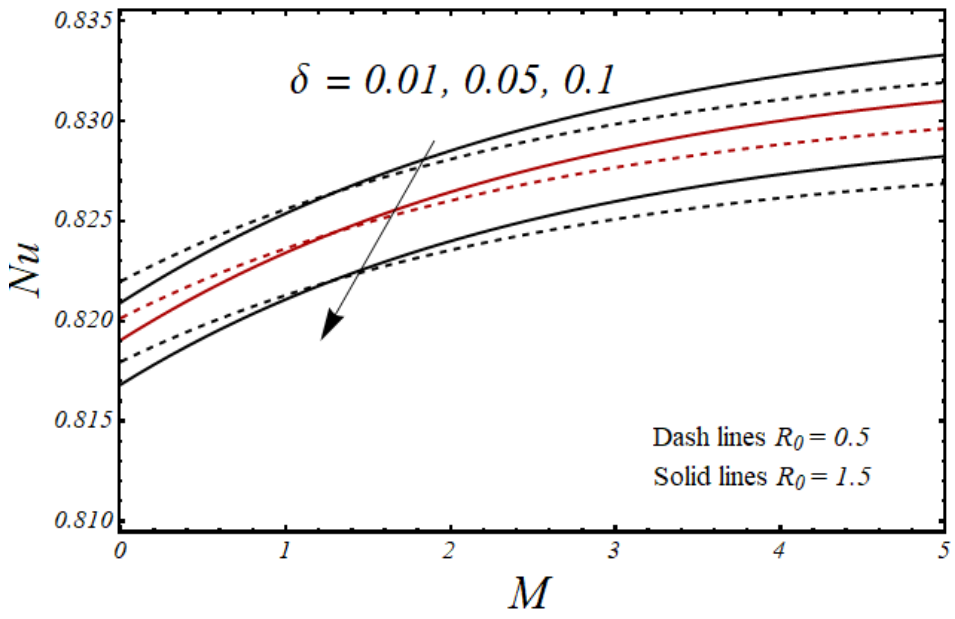

(a)

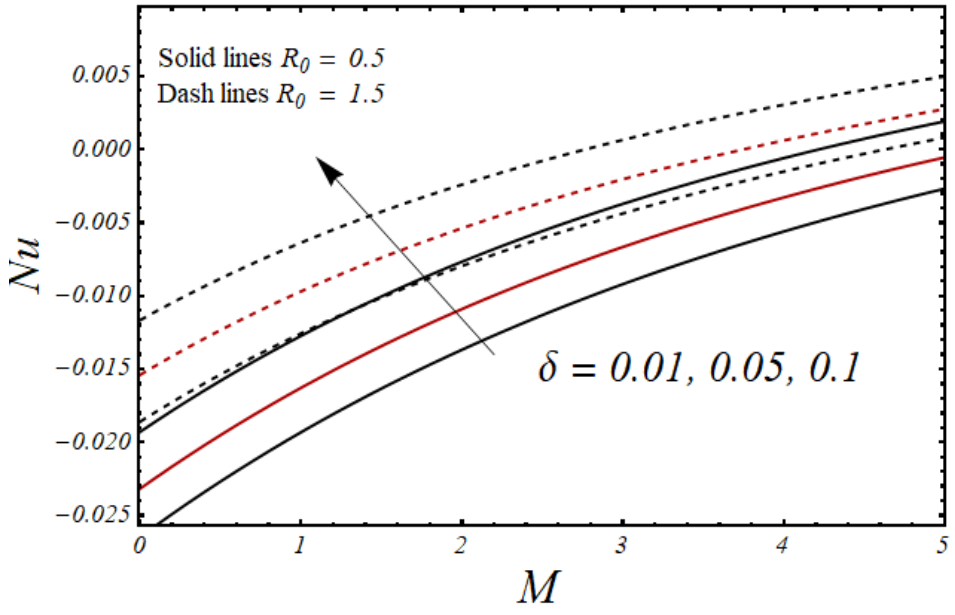

(b)

Figure 4.18: *Nu* with δ with R_0.

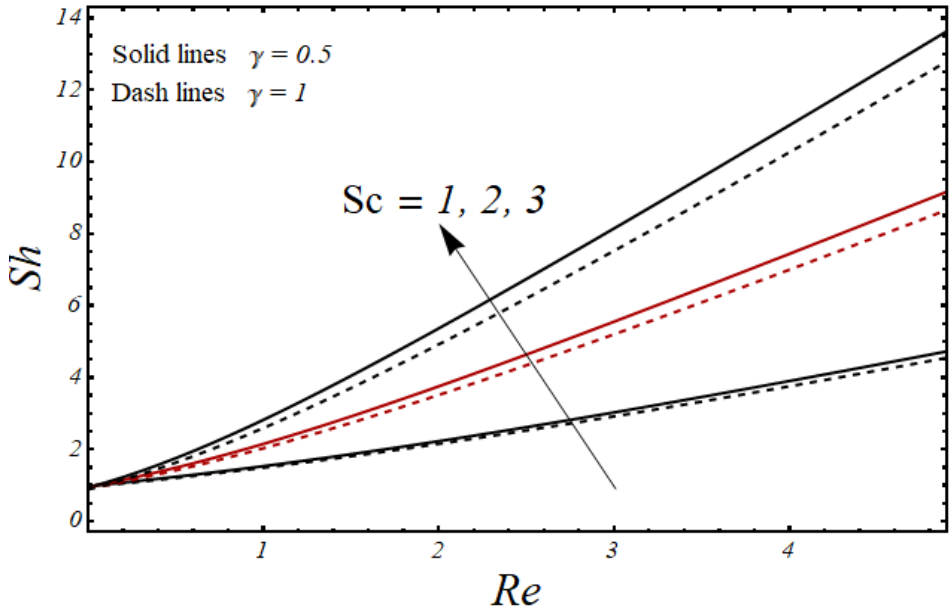

(a)

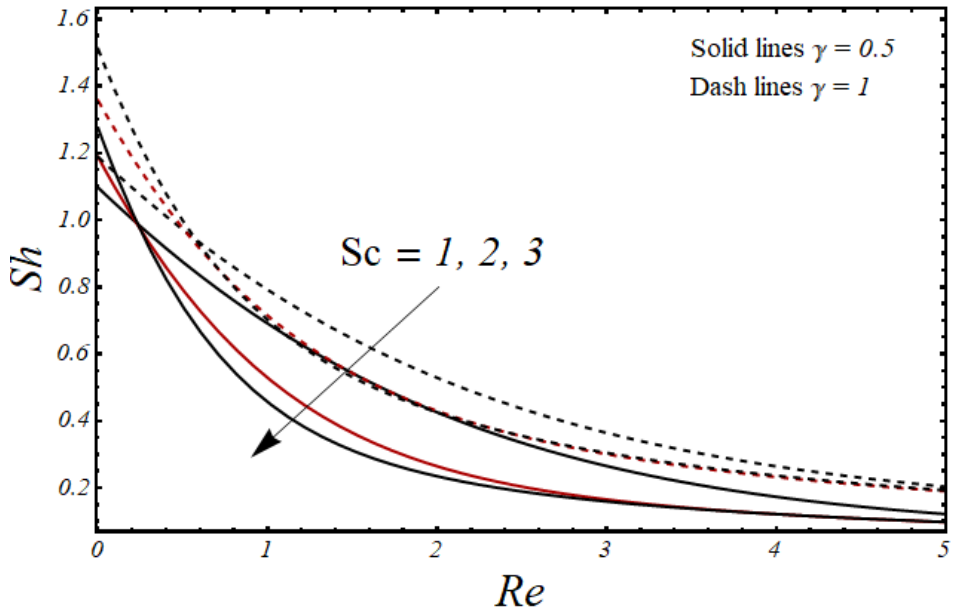

(b)

Figure 4.19: *Sh* with *Sc* and γ.

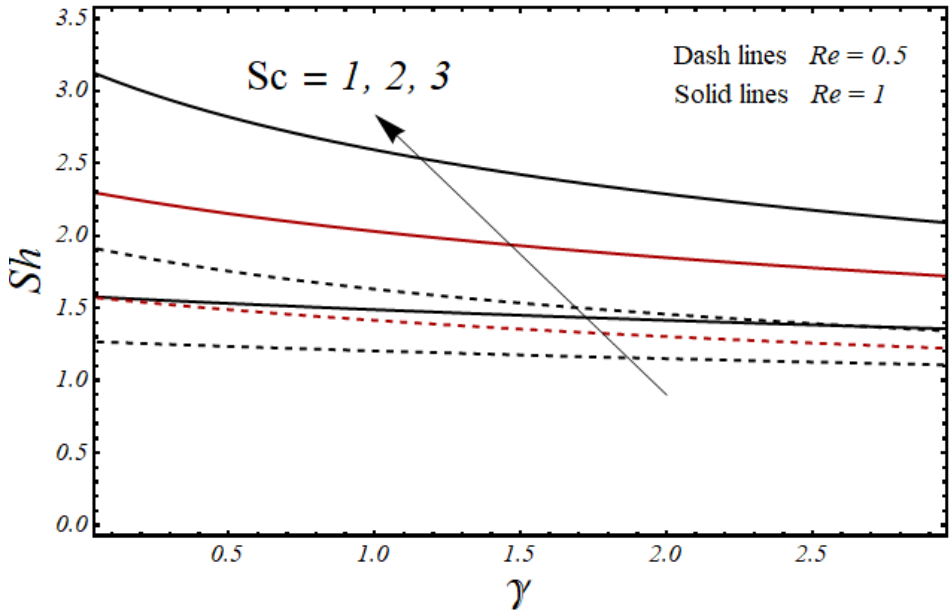

(a)

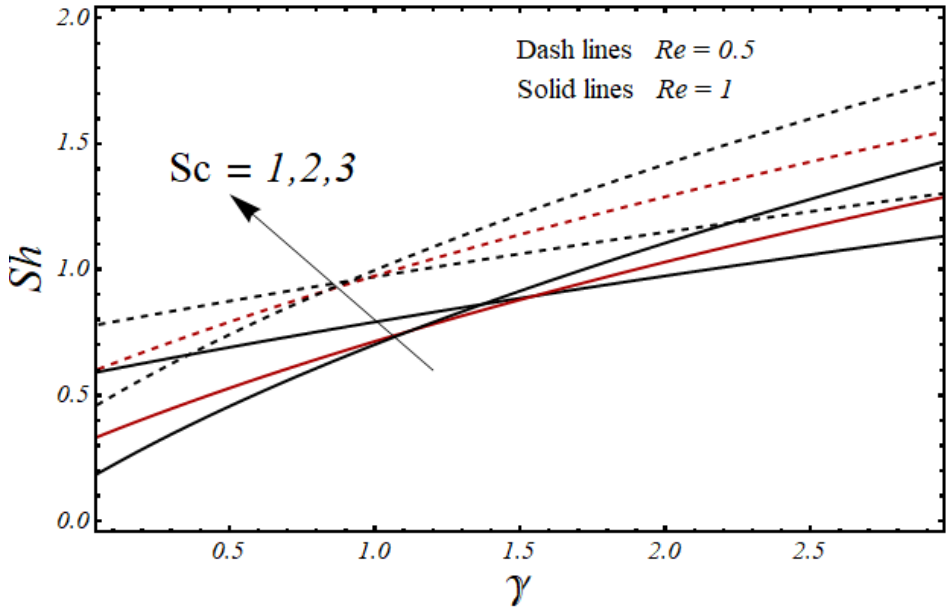

(b)

Figure 4.20: *Sh* with *Sc* and Re .

Chapter 5

Conclusion.

We extended our problem by considering CP flow of kerosene based FF in a rotating channel. By considering Tiwari & Das model in which the contribution of wall slip on the flow is also used in the presence of magnetic field whereas mass transfer analysis is carried out. The ferroparticles ($CoFe_2O_4$) are added to the based fluid (Kerosene). We examined the behavior of velocity, temperature and skin friction with help of different parameters i.e M, λ, Re, R_0, δ, Sc, γ and α . For solution of the equations we used some numerical methods i.e R-K and shooting. All the governing parameters on different fields are presented via graphs. Some momentous observations of this chapter 4 can be summarized as follows:

- $U(\eta)$ increased with λ , δ , M , Re , m and R_0 along with zero and non-zero slip parameter at the lower wall.
- $W(\eta)$ dncreased with λ , δ , M , Re , m and R_0 along with zero and non-zero slip parameter at the lower wall.
- Values of $U(\eta), W(\eta) \& \theta(\eta)$ are increased for greater values of φ and reduced for smaller values of φ with Re.
- The Cf_1 and Cf_2 increased with an increment of α and R_0 at lower surface whereas it reduced with the reduction of both parameter at upper surface for both primary and secondary flow.
- $\phi(\eta)$ enhanced by the greater value of Sc along with of γ.
- $\phi(\eta)$ is also increased by the increasing value of n and Re with the presence of Sc.

References

1. Choi, SUS, Enhancing thermal conductivity of fluids with nanoparticles, in: The proc. ASME Int. Mech. Eng. Cong. and Exp. ASME, San Francisco, USA. FED 231/MD, (1995) 66: 99-105.
2. Seo, HS, Lee, JC, Hwang, IJ, Kim, YJ, Flow characteristics of ferrofluid in a microchannel with patterned blocks, Material research Bulletin, (2014) 58:10-14.
3. Goharkhan, M, Ashajee, M, Effect of an alternating nonuniform magnetic field on ferrofluid flow and heat transfer in a channel, J. Magnetism and Magnetic Materials, (2014) 362:80-89.
4. Aminfar, H, Mohammad purfard, M, Maroofiazar, R, Experimental study on the effect of magnetic field on critical heat flux of ferrofluid flow boiling in a vertical annulus, Experimental Thermal and Fluid Sci, (2014) 58:156-169.
5. Murshed, SMS, Estelle, PA state of the art review on viscosity of nanofluids, Renewable and Sustainable Energy Reviews, (2017) 76:1134-1152.
6. Iftikhar, N, Rehman, A, Sadaf, H, Khan, MN, Impact of wall properties on the peristaltic flow of Cu-water nanofluid in a non-uniform inclined tube, Int. J. Heat and Mass Transfer, (2018)125:772-779.
7. Qiang, Xuan , Convective heat transfer and flow characteristics of Cu-nanofluid, School of Power Engineering, Nanjing University of Science and Technology, Nanjing 210094, China, (2002).
8. Sheikholeslami, M, Ganji, DD, Ferrohydrodynamic and magnetohydrodynamic effects on ferrofluid flow and convective heat transfer. Energy, (2014) 75: 400-410.
9. Sheikholeslami, M, Ganji, DD, Nanofluid flow and heat transfer between parallel plates considering Brownian motion using DTM. Comput. Methods. Appl. Mech. Engng., (2015) 283: 651-663.
10. Fakour, M, Vahabzadeh, A, and Ganji, DD, Study of heat transfer and flow of nanofluid in permeable channel in the presence of magnetic field. Propulsion and Power Research, (2015) 4(1): 50-62.
12. Attia HA, SayedAhmed, ME, Hall effect on unsteady MHD Couette flow and heat transfer of a Bingham fluid with suction and injection. Appl Math Model, (2004) 28(12):1027–45.
13. Priyadarsan K, Panda S, Flow and heat transfer analysis of magneto hydrodynamic (MHD) second-grade fluid in a channel with a porous wall. J Braz Soc Mec Sci Eng, (2017) 39(6):2145–57.
11. Mahmoodi, K, M, Kandelousi, Sh, Kerosene−alumina nanofluid flow and heat transfer for cooling application. J. Cent. South Univ, (2016) 23: 983−990.
14. Cramer, R, SI, Pai, Magnetofluid Dynamics for Engineers and Applied Physicists McGraw-Hill, NY, USA, (1973).

15. Rao, DRVP, Krishna, DV, Hall effects on free and forced convective flow in a rotating channel, Acta Mech, (1982) 43: 49–59.
16. Attia, HA, Effect of Hall current on transient hydromagnetic Couette–Poiseuille flow of a viscoelastic fluid with heat transfer, Appl. Math. Model, (2008) 32: 375–388.
17. Chauhan, DS, Agrawal, R, Effects of Hall current on MHD flow in a rotating channel partially filled with a porous medium, Chem. Eng. Commun, (2010) 197(6): 830–845.
18. Sarkar, BC, Das, S, Jana, RN, Combined effects of Hall currents and rotation on steady hydromagnetic Couette flow, Res. J. Appl. Sci. Eng. Technol., (2013) 5 (6): 1864–1875.
19. Jha, BK, Apere, CA, Combined effects of Hall current and ion-slip current on unsteady MHD Couette flow in a rotating system, J. Phy. Soci. Japan, (2010) 79 (10): (104401(1-9)).
20. Makinde, OD, Iskander, T, Mabood, F, Khan, WA, Tshehla, MS, MHD Couette-Poiseuille flowof variable viscosity nanofluids in a rotating permeable channel with Hall effects, Journal of Molecular Liquids 221, (2016) 778–787.
21. Fang, X, Xuan, Y, Qiang Li, Experimental investigation on enhanced mass transfer in nanofluids, Appl. Phys. Lett., (2009).
22. Seth, GS, Nandkeolyar, R, MHD Couette Flow in a Rotating System in the Presence of an Inclined Magnetic Field, Applied Mathematical Sci., (2009) 3:2919 – 2932.
23. Serna, J, Heat and mass transfer mechanisms in nanofluids boundary layers, Int. J. Heat and Mass transfer, (2016) 92:173-183.
24. Gurminder, S, Chamkha, AJ, Dual solutions for second-order slip flow and heat transfer on a vertical permeable shrinking sheet, Ain Shams Engineering Journal, (2013) 4, 911–917.
25. Ojjela, O, Kumar, NN, Unsteady heat and mass transfer of chemically reacting micropolar fluid in a porous channel with hall and ion slip currents. Int. Sch. Res. Notices, (2014) Article ID 646957.
26. Fakour, M, Vahabzadeh, A, Ganji, DD, Hatami, M, Analytical study of micropolar fluid flow and heat transfer in a channel with permeable walls. J. Molec. Liq., (2015) 204: 198-204.
27. Tetbirt, A, Bouaziz, MN Abbes, MT, Numerical study of magnetic effect on the velocity distribution field in a macro/micro – scale of a micropolar and viscous fluid in a vertical channel, J. Molec. Liq., (2016) 216: 103-110.
28. Ali, A, Ashraf, M, Ahmed, S, Batool, K, Viscous Dissipation and Radiation Effects in MHD Stagnation Point Flow towards a Stretching Sheet with Induced Magnetic Field, W.App.Sci. J., (2012): 16(11)1638-1648.
29. Makinde, OD, Onyejekwe OO, A numerical study of MHD generalized Couette flow and heat transfer with variable viscosity and electrical conductivity, J. Magn. Magn. Mater, (2011) 323: 2757–2763.

30. Das, S, Mandal, HK, Jana, RN, Makinde, OD, Magneto-nanofluid flow past an impulsively started porous flat plate in a rotating frame, J. Nanofluids, (2015) 4: (2) 167–175.
31. Makinde, OD, Effects of viscous dissipation and Newtonian heating on boundary layer flow of nanofluids over a flat plate, Int. J. Numer. Methods Heat Fluid Flow, (2013) 23:(8) 1291–1303.
32. Abbas,Z, Naveed, M, Sajid, M, Hydromagnetic slip flow of nanofluid over a curved stretching surface with heat generation and thermal radiation, J. Mol. Liq., (2016) 215: 756–762.
33. Das, S, Jana, RN, Makinde, OD, Mixed convective magneto hydrodynamics flow in a vertical channel filled with nanofluids, Eng. Sci. and Tech., Int. J., (2015) 18:244-255.
34. Baag, S, Mishra, SR, Dash, CC, Acharya, MR, Entropy generation analysis for viscoelastic MHD flow over a streching sheet embeded in a porous medium, Ain Shams Eng. J., (2017) 8:623-632.
35. Fersadou, I, Kahalerras, H, Ganaoui, El, M, MHD mixed convection and entropy generation of a nanofluid in a vertical porous channel, Computers & Fluids, (2015) 121:164-179.
36. Ibáñez, G, Entropy generation in MHD porous channel with hydrodynamic slip and convective boundary conditions, Int. J. Heat Mass Trans., (2015) 80:274–280.
37. Nandkeolyar, R, Narayana, M, Motsa, SS, Sibanda, P, Magnetohydrodynamic mixed convective flow due to a vertical plate with induced magnetic field, J. Thermal Sci. and Eng. Appli., (2018),Vol. 10, research-article.
38. Yuan, Ma, Rasul, Mohebbi, Rasul, Rashidi, MM, Zhigang Yang, Mikhail A, Sheremet, Numerical study of MHD nanofluid natural convection in a baffled U-shaped enclosure. Int. J. Heat Mass Trans., (2019) 130:123–134.
39. Wang, CY, Analysis of viscous flow due to a stretching sheet with surface slip and suction. Nonlinear Ana. Real World Appl., (2009) 10:375-380.
40. Aziz, A, Hydrodynamic and thermal slip flow boundary layer over a flat plate with constant heat flux boundary condition, Commun. Nonlinear Sci. Numer. Simul, (2010) 15:573-80.
41. Hayat, T, Qasim, M, Mesoub, S, MHD flow and heat transfer over permeable stretching sheet with slip conditions. Int. J. Numer. Methods Fluids, (2011) 66:963-975.
42. Abbas, Z, Rahim,T, Hasnain, J, Slip flow of magnetite-water nanomaterial in an inclined channel with thermal radiation, Int. J. Mech Sci., (2017) 122: 288-296.
43. Nandy, SK, Mahapatra, TR, Effects of slip and heat generation/absorption on MHD stagnation flow of nanofluid past a stretching/shrinking surface with convective boundary conditions. Int. J. Heat Mass Transf., (2013) 64:1091-1100.

44. Das, S, Jana, RN, Entropy generation due to MHD flow in a porous channel with Navier slip. Ain Shams Eng. J., (2014) 5(2): 575–584.
45. Sajid, M, Mahmood, R, Hayat, T, Finite element solution for flow of a third grade fluid past a horizontal porous plate with partial slip. Comp. Maths Appl., (2008) 56(5): 1236-1244.
46. Srinivasacharya, D, Kaladhar, K, Mixed convection flow of couple stress fluid between parallel vertical plates with Hall and Ion-slip effects. Commun Nonlinear Sci Numer Simulat, (2012) 17(6): 2447–2462.
47. Singh, G, Chamkha, AJ, Dual solutions for second-order slip flow and heat transfer on a vertical permeable shrinking sheet. Ain Shams Eng. J., (2013) 4: 911-917.
48. Sajid, M, Ali, N, Abbas, Z, Javed, T, Stretching flows with general slip boundary condition. Int. J. Modern Phy. B, (2010) 24: 5939-5947.
49. Rao, AS, Prasad, VR, Reddy, NB, Anwar BO, Heat Transfer in a Casson Rheological Fluid from a Semi-infinite Vertical Plate with Partial Slip. Heat Transf. Asian Res (2008).
50. Nandy, SK, Mahapatra, TR, Effects of slip and heat generation/absorption on MHD stagnation flow of nanofluid past a stretching/shrinking surface with convective boundary conditions. Int. J. Heat Mass Transf., (2013) 64: 1091-1100.
51. Khan, WA, Makinde, OD, Khan, ZH, Non-aligned MHD stagnation point flow of variable viscosity nanofluids past a stretching sheet with radiative heat, Int. J. Heat Mass Transf., (2016) 96: 525–534.